

ספריות הטכניון *The Technion Libraries*

בית הספר ללימודי מוסמכים ע"ש ארווין וג'ואן ג'ייקובס
Irwin and Joan Jacobs Graduate School

©

All rights reserved to the author

This work, in whole or in part, may not be copied (in any media), printed, translated, stored in a retrieval system, transmitted via the internet or other electronic means, except for "fair use" of brief quotations for academic instruction, criticism, or research purposes only. Commercial use of this material is completely prohibited.

©

כל הזכויות שמורות למחבר/ת

אין להעתיק (במדיה כלשהי), להדפיס, לתרגם, לאחסן במאגר מידע, להפיץ באינטרנט, חיבור זה או כל חלק ממנו, למעט "שימוש הוגן" בקטעים קצרים מן החיבור למטרות לימוד, הוראה, ביקורת או מחקר. שימוש מסחרי בחומר הכלול בחיבור זה אסור בהחלט.

**Non Equilibrium Statistical Mechanics:
Electric Networks, Energy Forms and
the Additivity Principle**

Ohad Shpielberg

**Non Equilibrium Statistical Mechanics:
Electric Networks, Energy Forms and
the Additivity Principle**

Research thesis

**In Partial Fulfillment of the
Requirements for the Degree of Doctor
of Philosophy**

Ohad Shpielberg

**Submitted to the Senate of the
Technion - Israel Institute of Technology**

Sivan, 5774 Haifa July, 2016

The Research Thesis Was Done Under the Supervision
of Professor Eric Akkermans in the
Department of Physics

The Generous Financial Help of The Technion
is Gratefully Acknowledged

Contents

List of Figures	i
List of Tables	iii
Abstract	1
List of Symbols	3
1 Introduction	7
2 The Macroscopic Fluctuations Theory	9
3 Current Fluctuations	13
3.1 Current Fluctuations	13
3.2 Le Chatelier Principle	15
3.3 Stability of Hamiltonian Systems	17
3.4 Validity of the Additivity Principle	19
3.4.1 The validity of the additivity principle for systems under a weak applied field	20
3.5 Applications	21
3.5.1 The Weakly Asymmetric Exclusion Process	21
3.5.2 The KMP Process	21
3.6 Remarks on dynamical phase transitions	24
4 Universal Current Fluctuations	27
4.1 Universality of the CGF	27
4.2 Energy Forms	29
4.3 Numerical Results	30
5 The MFT and Quantum Transport	35
5.1 Langevin Approach to Mesoscopics	35
5.2 Density Correlations	37
5.3 Applications	39
5.3.1 Intensity Fluctuations of Coherent Light and the KMP	39

5.3.2	Electron Transport Through a Disordered Conductor and the SSEP	41
5.4	Overview	44
6	Summary	45
A	Numerical Methods	47
	Bibliography	51

List of Figures

2.1	Asymmetry in a microscopic model	11
3.1	λ to J conversion	23
3.2	Stability analysis in the currents plain for the KMP model	23
3.3	Stability analysis in the Fourier plain the KMP model	24
4.1	The graphs of the first group	30
4.2	Fano factor and second Fano factor convergence for the first group	31
4.3	Finite size corrections for the Fano factor and the second Fano factor	32
4.4	Graphs of the second group	33
5.1	Electronic transport through a dirty conductor	41
5.2	Fermi-Dirac distribution function for the two reservoirs	42

List of Tables

4.1	Scaling exponents for the finite size corrections	32
4.2	Cumulants of the SSEP on the second group graphs	34

Abstract

Systems with many degrees of freedom are notoriously hard to grasp intuitively as well as capture mathematically. Thermodynamics and statistical mechanics ideas allowed for a leap in the understanding of such complex systems at equilibrium over a century ago. Despite this success, little is known when our system is taken out of equilibrium. Moreover, most of the knowledge concentrates on system driven slightly out of equilibrium.

In the last 15 years, the macroscopic fluctuation theory was shown to be a successful description of out of equilibrium diffusive systems. It was shown to successfully capture the behavior of the few solvable models in the field. In this Thesis, I will focus on the study of two properties of diffusive boundary driven systems within the scope of the macroscopic fluctuation theory.

The first, current fluctuations, allows intuitive understanding of the physics governing the system through the noise statistics of the steady state. Generally, calculating the current fluctuations is hard. However, a clever guess, known as the additivity principle, allows to obtain analytically an expression for the current fluctuations. This Thesis presents a sufficient and necessary condition for the validity of the additivity principle guess. Moreover, assuming the validity of the additivity principle, the universality of current fluctuations is shown for systems of arbitrary geometry.

The second property discussed is the density correlations. While in equilibrium - away from a phase transition, correlation functions are known to decay exponentially, for systems driven out of equilibrium, correlation functions are generically long ranged. Using known results for diffusive classical systems, it is shown that transport in disordered quantum systems can also be studied using the macroscopic fluctuation theory. Moreover, an exact correspondence between classical processes and some quantum processes is found.

List of Symbols

α, β	scaling exponents
$\bar{\rho}$	the density profile solution under the AP
$\bar{F}^\#$	numerical value of the Fano factor
\bar{F}^\star	evaluation of the Fano factor
$\delta\rho$	density fluctuation
δj	current fluctuation
δs_{AP}^2	the integrand of the variation of the action under the AP
δV	A voltage drop
Δ	a Laplacian
Δ^{-1}	the inverse Laplacian operator
η	a white noise term
γ	a complex number
$\hat{\rho}$	density profile
\hat{v}	a vector of density and momentum fluctuations
λ	the cumulant generating function parameter
\mathbb{C}	the complex plain
\mathbf{x}	A position vector in d dimensions
\mathcal{F}	the large deviation functional
\mathcal{G}	a pressure functional
\mathcal{H}	a Hamiltonian
$\mathcal{H}_{\rho\rho}$	Second functional derivative of \mathcal{H} with respect to ρ

\mathcal{H}_{pp}	Second functional derivative of \mathcal{H} with respect to p and ρ
\mathcal{H}_{pp}	Second functional derivative of \mathcal{H} with respect to p
\mathcal{L}	Lagrangian density
$\mathcal{P}_t(Q)$	probability to observe a transfer of Q particle in time t
$\mathcal{R}, \mathcal{R}_x, \mathcal{R}_y$	elliptic operators
\mathcal{R}^\dagger	an adjoint operator
$\mu(\lambda)$	Cumulant generating function
μ_1	the CGF of $1d$ chain of sites
μ_G	the CGF of the graph G
ν	Density of states
ω	The frequencies of the Fourier decomposition of the fluctuations
ω_0	A frequency of the Fourier decomposition of the fluctuations
\bar{I}	numerical mean current
Φ	the large deviation function
Π	the momentum conjugate to the density profile
ρ	density
ρ_a, ρ_b	reservoir densities
ρ_l, ρ_r	reservoir densities
ρ_s	the steady state density profile
σ	conductivity
σ_0	σ evaluated at the AP density profile
$\sum_{j \sim i}$	summation over all the neighbors j of the site i
τ	diffusively scaled time coordinate
\tilde{s}	A smooth function
A	a vector potential
a	an operator
A_f	auxiliary function
B_f	auxiliary function

C_f	auxiliary function
C_{eff}	an effective conductance
C_n	the density correlation function of order n
c_{xy}	capacitance of the xy bond
D	diffusion
d	dimensionality of the system
D_0	σ evaluated at the AP density profile
E	applied field
e	a charge
E_G	the energy of the graph G
F, F_2	the first and second Fano factors
$f_\omega, \bar{f}_\omega, \hat{f}_\omega$	a Fourier ω mode of the $\delta\rho$ fluctuation.
$g_\omega, \bar{g}_\omega, \hat{g}_\omega$	a Fourier ω mode of the δp fluctuation.
H	the Hamiltonian conjugate to the LDF under the AP
h	auxiliary function
J	a constraint current
j	current
J_c	critical current
J_s	the steady state current
L^\star	effective number of sites
$L^\#$	numerical evaluation of effective number of sites
l_e	mean free path
m	effective mass
n_i	occupancy of particles at site i
p	Lagrange multiplier conjugate to the continuity equation
Q	Number of particles
$q_{i,j}$	the integrated current from site i to site j
S	the action of the cumulant generating function

s	the integrand of the action
U	the LDF with the AP
V	the potential of the Hamiltonian
$v(\mathbf{x})$	A continuous potential function
V_i	A discrete potential function
v_e	group velocity
x	diffusively scaled space coordinate
AP	Additivity principle
CGF	Cumulant generating function
KMP	Kipnis, Marchioro and Presutti
L	system size
LDF	Large deviation function
MFT	Macroscopic fluctuation theory
Q	integrated current
SSEP	simple symmetric exclusion process
t	time
WASEP	weakly asymmetric exclusion process

Chapter 1

Introduction

Statistical mechanics and thermodynamic ideas proved successful enough, that their use is ubiquitous in every field of exact science. This allows to hide the fact that most processes are taking place out of equilibrium, where only a few and limited results are known. Spanning from living biological systems, geophysical processes in the earth's core, gel physics and the evolution of the universe itself, the study of equilibrium physics is limited to building clever and simple models without any unifying theory. Despite the clear interest, the field is lacking not only in an encompassing theory on the scale of statistical mechanics or thermodynamics, but also in a clear definition of its boundaries. A major step towards both these goals and one of the prominent successes of mathematical physics has been the formulation of the macroscopic fluctuation theory (MFT). The MFT, successfully describes the macroscopic fluctuations in the non-equilibrium steady state, thus allowing to account for various important phenomena, e.g. current fluctuations, non-equilibrium density correlations, emergence or decay of rare fluctuations, etc. The fundamental formula of the MFT is the probability of observing a current $j(x, \tau)$ and density $\rho(x, \tau)$ fluctuations in an out-of-equilibrium system, within some finite time window.

The general notion one pertains is that out of equilibrium physics is model dependent and looking for universal behavior is doomed to failure. In this Thesis, we will focus on boundary driven processes within the framework of the MFT. Using the MFT, we analyze problems from a general perspective, later applying them to specific models. This allows to derive universal results as well as understanding generic behavior. Moreover, the application of general results allows to understand that the MFT captures the behavior of mesoscopic systems, so far not considered within the scope of the MFT.

The outline for this Thesis is the following.

In Chapter 2, we use a Langevin like approach to derive the MFT. This allows to describe the steady state current and density fluctuations. The probability to observe such fluctuations is given in terms of an action, like the description with a Lagrangian formalism.

In Chapter 3, we use the MFT to characterize the current fluctuations, where

one is interested in the probability of observing an atypical current during a large time window. Taking advantage of a corresponding Hamiltonian description of the MFT, we are able to formulate a criterion for dynamical phase transitions in current fluctuations. These phase transitions show explicit breaking of time translational symmetry. Since the observation of a macroscopically atypical current is exponentially unlikely for large systems, we generally do not expect to observe such dynamical phase transitions except in the case of critical systems.

In Chapter 4, the results of Chapter 3 are used to show that in the case no explicit breaking of time translational symmetry is found, current fluctuations are universal with respect to the geometry of the system and we recover a generalization of Kirchhoff rules for resistors/capacitors for current fluctuations. This generalization expands potential theory beyond the mean current.

In Chapter 5, it is shown that using the Langevin approach, the MFT can be shown to successfully describe transport in models of mesoscopic disordered quantum systems. We present two such examples of mesoscopic processes where there is a classical analog process.

Chapter 2

The Macroscopic Fluctuations Theory

The purpose of this mathematical introduction, is to derive the MFT expression for the probability distribution using a Langevin equation for diffusive processes. One can also derive the probability distribution using first principles in two different approaches [1, 2], however, for our purpose, the Langevin method is preferable. Let us restrict ourselves to a one-dimensional system for the sake of simplicity. A generalization for higher dimensions is straightforward. Consider a lattice gas, such that $n_i(t')$, $i \in 1, \dots, L$ denote the time-dependent occupancies of the $L \gg 1$ sites of the system evolving in the time interval $[0, t]$. Throughout this text, we consider only non-dissipative dynamics, such that particles may be created or annihilated only at the boundaries. The system may be driven out of equilibrium by initial conditions, or by fixing boundary conditions, e.g. periodic boundary conditions or fixed density at the boundaries. Here, we wish to focus on the latter case. The coupling of the system to two reservoirs proves useful in the formulation and understanding of the Langevin equation. To compose a macroscopic picture, one needs to account for the macroscopic observables. In the simplest case (one species of particles), the observables are the density profile $\rho_i(t)$ and the particles flux $Q_i(t)$ at site i in the time window $[0, t]$. The continuity equation reads $\partial_t \rho_i(t) = -\partial_i j_i(t)$, where $j_i(t) = \partial_t Q_i(t)$ is the current. However, to obtain a consistent diffusive macroscopic picture, we introduce the rescaled coordinates $x = i/L$ and $\tau = t/L^2$ such that in the large system size $L \rightarrow \infty$ and large times $t \rightarrow \infty$ limits, we keep $t/L^2 \rightarrow \text{const}$. It is therefore convenient to define a rescaled density $\rho(x, \tau) = \rho_i(t)$ and particle flux $Q(x, \tau) = LQ_i(t)$ such that the rescaled continuity equation becomes $\partial_\tau \rho(x, \tau) = -\partial_x j(x, \tau)$.

For such a system, coupled to two reservoirs with fixed densities $\rho_{l,r}$ at the right (left) boundary¹, we assume the existence of a steady state with a corresponding steady state density profile $\rho_s(x)$ and steady state current J_s .

¹This fixes the boundary conditions $\rho(x=0, \tau) = \rho_l$, and $\rho(x=1, \tau) = \rho_r \forall \tau$.

We further assume Fick's law, $J_s = -D(\rho_s) \partial_x \rho_s$. Applying the continuity equation

$$\partial_\tau \rho = -\partial_x j \quad (2.1)$$

allows to identify the diffusion coefficient D . The diffusion D typically depends on the density profile when the process includes interactions between the particles (see [3] for an example).

Next, we build on Fick's law, and describe a current and density fluctuation $j(x, \tau), \rho(x, \tau)$ using a Langevin equation

$$j(x, \tau) = -D(\rho(x, \tau)) \partial_x \rho(x, \tau) + \sqrt{\frac{\sigma(\rho(x, \tau))}{L}} \eta(x, \tau), \quad (2.2)$$

with a weak (i.e. $1/\sqrt{L}$) noise, where η is a white noise term such that

$$\begin{cases} \langle \eta(x, \tau) \rangle = 0 \\ \langle \eta(x, \tau) \eta(x', \tau') \rangle = \delta(x - x') \delta(\tau - \tau'), \end{cases}$$

and $\sigma(\rho)$ is its strength. Here, $\langle \cdot \rangle$ denotes averaging with respect to the steady state distribution (yet to be defined). It is not very convenient to work with the Langevin equation. Therefore, it is useful to obtain a path integral formulation using the Martin-Siggia-Rose procedure [4]. It allows to write the (steady state) probability distribution to observe a density and current fluctuation during a time window $[0, t/L^2]$, namely

$$P_t(\{j, \rho\}) \sim \exp \left[-L \int_0^1 dx \int_0^{t/L^2} d\tau \mathcal{L}(j, \rho) \right] \quad (2.3)$$

with

$$\mathcal{L}(j, \rho) = \frac{(j + D(\rho) \partial_x \rho)^2}{2\sigma(\rho)}, \quad (2.4)$$

subjected to the continuity equation $\partial_\tau \rho + \partial_x j = 0$. It is noteworthy to mention that D and σ are not independent but obey the Einstein relation $\sigma/2D = \chi(\rho)$, where χ is the equilibrium compressibility. It is a surprising relation since D and σ as defined, describe the far from equilibrium fluctuations in the system. The Einstein relation also allows to identify σ as the conductivity of the system in the corresponding case.

One may also consider applying a microscopic asymmetry between the right/left hopping rates $E/2L$ (see for example Figure 2.1). Using fluctuation-dissipation relation, one can show that the Langevin equation (2.2) rewrites

$$j(x, \tau) = -D(\rho(x, \tau)) \partial_x \rho(x, \tau) + \sigma(\rho(x, \tau)) E + \sqrt{\frac{\sigma(\rho(x, \tau))}{L}} \eta(x, \tau). \quad (2.5)$$

Therefore, in the path integral (2.4) becomes

$$\mathcal{L}(j, \rho) = \frac{(j + D(\rho) \partial_x \rho - \sigma E)^2}{2\sigma(\rho)}. \quad (2.6)$$

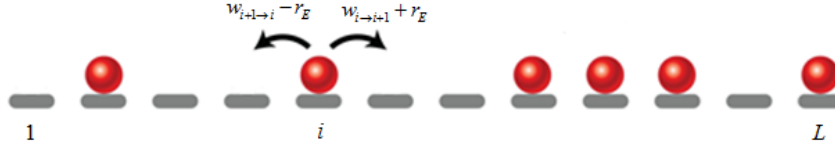


Figure 2.1: In this microscopic model, we have L sites. We introduce symmetric jump rates $w_{i \rightarrow j}$ between neighboring sites i and j , where $w_{i \rightarrow j}$ do not depend on the direction of the jump. We also include an asymmetric rate, $r_E = E/2L$ which increases the jump rate to the right (for positive E) and decreases the rate to the left.

In the above, we have derived the probability to observe a fluctuation in an out of equilibrium system. This is the main result of the MFT, and while it was rigorously proven for lattice gas models [5, 6, 7], its range of validity seems to extend beyond that case [8, 9, 2]. In the next Chapter, we will focus on current fluctuations, an important quantity used to characterize out of equilibrium systems. Nevertheless, it must be emphasized that the MFT is not limited to calculation of current fluctuations [10, 11, 12, 13, 14, 15]. This will be developed in the next chapters.

Chapter 3

Current Fluctuations

In this Chapter, we take advantage of a resulting time translational symmetry in order to evaluate the current fluctuations using a Hamiltonian formalism. Using thermodynamic ideas, we discuss the possibility of breaking the time invariance symmetry which is interpreted as a dynamical phase transition.

3.1 Current Fluctuations

Among the various applications of the MFT, we will focus here on current fluctuations for boundary driven systems. Current fluctuations define a measure of the distance of an atypical current from the steady state and provides useful information about the physics of the system [16]. We will present a way to analytically evaluate the current fluctuations.

We define by Q the number of particles flowing during a time window $[0, t/L^2]$, from the left hand side reservoir to the right hand side reservoir. In our macroscopic language, one can obtain Q using

$$Q = L^2 \int dx d\tau j(x, \tau), \quad (3.1)$$

where we have assumed that no accumulation of particles takes place in the bulk (otherwise see [17, 18]). In the long time limit, one assumes a large deviation principle for the probability distribution $\mathcal{P}_t(Q)$,

$$\mathcal{P}_t(Q) \sim e^{-t\Phi(Q/t)}, \quad (3.2)$$

where Φ , known as the large deviation function (LDF), is a scaling function of Q/t [19]. To obtain a formal expression of Φ , we use the MFT probability distribution (2.3), and sum over all possible fluctuations $\{j(x, \tau), \rho(x, \tau)\}$ that satisfy (3.1) and the continuity equation (2.1), namely

$$\mathcal{P}_t(Q) \sim \int \mathcal{D}j \mathcal{D}\rho \exp \left[-L \int dx d\tau \mathcal{L}(j, \rho) \right] \delta \left(Q - L^2 \int dx d\tau j \right) \delta(\partial_\tau \rho + \partial_x j). \quad (3.3)$$

For a large system size $L \gg 1$, we can use a saddle point approximation to evaluate (3.3). Thus, we find that there is an optimal fluctuation $\{j, \rho\}$ that dominates $\mathcal{P}_t(Q)$. However, due to the two constraints, i.e. the integrated current (3.1) and the continuity equation (2.1), finding the optimal fluctuation $\{j, \rho\}$ is a hard minimization problem. The additivity principle (AP), proposed by Bodineau and Derrida [20], assumes that this dominant density fluctuation is time-independent and that the optimal current fluctuation has a fixed¹ $J = Q/t$. It is straightforward to verify that the AP solution satisfies the two constraints (2.1),(3.1) such that the minimization problem becomes simpler. From (3.2) and (3.3) one finds

$$U(J) = \frac{1}{L} \inf_{\rho(x)} \int dx \mathcal{L}_J(\rho, \partial_x \rho), \quad (3.4)$$

with $\mathcal{L}_J(\rho, \partial_x \rho) = (J + D(\rho) \partial_x \rho)^2 / 2\sigma(\rho)$ and $U(J)$ is the LDF under the AP assumption. It is easy to verify that $U(J)$ is an upper bound for the LDF $\Phi(J)$. The minimization problem in (3.4) is an Euler-Lagrange problem, with substitution of the usual integration w.r.t. time by an integration w.r.t. space. Therefore, the optimal density fluctuation $\bar{\rho}(x)$ is the solution of the Euler-Lagrange equation $\frac{\delta \mathcal{L}_J}{\delta \rho} = \frac{d}{dx} \frac{\delta \mathcal{L}_J}{\delta \partial_x \rho}$, which reads,

$$\partial_{xx} \bar{\rho} + \left\{ \frac{D'(\bar{\rho})}{D(\bar{\rho})} - \frac{\sigma'(\bar{\rho})}{2\sigma(\bar{\rho})} \right\} (\partial_x \bar{\rho})^2 + \frac{\sigma'(\bar{\rho})}{2D^2(\bar{\rho})\sigma(\bar{\rho})} J^2 = 0. \quad (3.5)$$

Thus, the calculation of the LDF using the AP, boils down to solving (3.5), a boundary value, second order non-linear ordinary differential equation. This is a major simplification compared to the original problem².

Setting aside the mathematical convenience of the AP, the suggested solution may appear to be an odd guess. This time-independent guess should be completely unnatural for a system far from equilibrium and constrained to exhibit an atypical particle flux (that can even be against the direction of the steady state current). Despite these remarks, the AP assumption proved to be exact for several important models [20, 22, 23, 24, 25, 26, 27]. It is thus interesting (and useful) to find a physical interpretation and further justification for the use of the AP.

Recall that (3.4) and (3.5) are expressions resulting from a Lagrangian formalism. Therefore, it is worthwhile to employ the conjugate Hamiltonian formalism. The Legendre transform $H(\rho, \Pi) = \Pi \partial_x \rho - \mathcal{L}_J(\rho, \partial_x \rho)$, with $\Pi = \frac{\delta \mathcal{L}_J}{\delta \partial_x \rho}$ gives

$$H(\rho, \Pi) = \frac{1}{2m(\rho)} [\Pi - eA(\rho)]^2 + V(\rho), \quad (3.6)$$

¹Since we are interested in the long time limit, we are not concerned with a macroscopically negligible time scale where the system adjusts itself to the optimal solution.

²Notice that the optimal density profile is symmetric about $J \rightarrow -J$. This symmetry is at the basis of the well known Gallavotti-Cohen relation [21], a benchmark for out of equilibrium systems.

where

$$\begin{cases} m(\rho) = D^2/\sigma \\ A(\rho) = D/\sigma \\ V(\rho) = -e^2/\sigma \\ e = J. \end{cases}$$

This Hamiltonian representation allows to formulate the many-body, constrained and out of equilibrium problem as a single particle problem in a weird potential and effective mass. Moreover, as the Hamiltonian does not depend explicitly on the spatial coordinate x , the energy density H is a conserved quantity. This implies that the AP assumption is merely an assumption about a spatially uniform energy of the system. Spatial uniformity of the energy is a consequence of thermodynamics and characterizes systems at equilibrium. It is therefore useful to consider thermodynamical tools to address this problem, and to consider the LDF as an out of equilibrium generalization of a thermodynamic potential [28]. This allows to explore the range of validity of the AP and many more familiar thermodynamic ideas. Since we have assumed a unique steady state for our boundary driven system, the AP is valid for $J = J_s$. Therefore, it is plausible to assume that there is always some finite region for which the AP applies. Far from the steady state current J_s , one may consider a finite J_c , beyond which the AP is no longer valid. In this case, the energy density H will no longer be a “constant of motion” as in the Hamiltonian formalism. This leads to a spatial non-uniform energy distribution which resembles an equilibrium phase transition. Moreover, the symmetry breaking of the density profiles indicates a (second order like) phase transition. Thus it is convenient to coin dynamical phase transitions such a breaking of the AP at some critical current J_c .

3.2 Le Chatelier Principle

The last section implies that it is useful to borrow thermodynamic concepts in order to gain knowledge of current fluctuations. In thermodynamics, the Le Chatelier principle allows to discuss the stability of phases. In short, it states that starting from a system at equilibrium, any fluctuation leads back to the equilibrium state. This is a restatement of the fact that thermodynamic potentials are convex. The natural generalization for out of equilibrium systems is to require that the optimal solution of the LDF yields a convex function with respect to all possible fluctuations $\delta j, \delta \rho$. Then, to extend the idea underlying the Le Chatelier principle to the LDF, we require the convexity of $\int dx d\tau \mathcal{L}(J, \bar{\rho})$, where $\bar{\rho}(x)$ is the AP solution of (3.5), namely

$$\int d\tau dx \{ \mathcal{L}(J + \delta j, \bar{\rho} + \delta \rho) - 2\mathcal{L}(J, \bar{\rho}) + \mathcal{L}(J - \delta j, \bar{\rho} - \delta \rho) \} \geq 0, \quad (3.7)$$

where the fluctuations $\delta j, \delta \rho$ must satisfy the continuity equation $\partial_\tau \delta \rho = -\partial_x j$, the boundary conditions, $\delta \rho(x=0, \tau) = \delta \rho(x=1, \tau) = 0 \forall \tau$, and not to con-

tribute any excess integrated current; namely $\int dx d\tau \delta j(x, \tau) = 0$. Mathematically, the Le Chatelier principle translates into a requirement that the extremal AP solution (for a time independent density profile), is also a minimal solution (in the larger space of all the allowed currents and density fluctuations). In Le Chatelier language, breaking of (3.7) translates into a dynamical phase transition, as discussed above. In what follows we consider only continuous dynamical phase transitions, where for some critical current J_c , the optimal trajectory smoothly changes from the AP solution $\{J, \bar{\rho}(x)\}$ to a time dependent one $\{J + \delta j(x, \tau), \bar{\rho}(x) + \delta \rho(x, \tau)\}$. In that case, somewhat analogous to a second order phase transition, one can expand (3.7) perturbatively for small fluctuations $\delta j, \delta \rho$. This approach proves useful for systems with periodic boundary conditions, $\rho(x=0, \tau) = \rho(x=1, \tau)$ where the particle number is conserved [29, 30, 31] and exact simulations confirmed these findings [32, 33]. In [34], it was found that a sufficient and necessary condition for the validity of the AP in periodic systems corresponds to $\sigma'' \leq 0$ ³⁴. However, for boundary driven systems, it seems that this approach leads to a dead end [29]. This is the result of the spatial non-uniformity in the boundary driven case (as opposed to the periodic case). Thus, one cannot write (3.7) as a suitable quadratic diagonal form for a general D and σ .

In thermodynamics, we are used to the fact that choosing the right thermodynamic potential is essential, e.g. calculating the Gibbs free energy vs. the Helmholtz free energy for black body radiation [35, 36]. This notion turns out to be just as important for calculating LDFs. Let us define $\mu(\lambda)$, the Cumulant Generating Function (CGF) for the current fluctuations,

$$\mu(\lambda) = \lim_{t \rightarrow \infty} \frac{1}{t} \log \left\langle e^{\lambda Q/L} \right\rangle_{\mathcal{P}_t(Q)},$$

where the averaging is with respect to $\mathcal{P}_t(Q)$. It is easy to verify that

$$\frac{\partial^n \mu(\lambda)}{\partial \lambda^n} \Big|_{\lambda=0} = \frac{\langle Q^n \rangle_C}{t},$$

where $\langle Q^n \rangle_C$ is the n -th cumulant. Moreover, using the large deviation principle (3.2), it is straight forward to verify that μ is a Legendre transform of the LDF $\Phi(J)$ ⁵

$$\mu(\lambda) = -\frac{1}{L} \inf_J \{L\Phi(J) - \lambda J\}. \quad (3.8)$$

It should be clear that the CGF and the LDF contain the same information. The CGF is a particularly useful tool to study current fluctuations as it relaxes the integrated current constraint (3.1), and introducing a Lagrange multiplier p , relaxes the continuity equation constraint (2.1). The CGF can be formulated

³Hereafter the O' will be used as a differentiation with respect to the density, e.g. $\sigma' \equiv \frac{d\sigma}{d\rho}$.

⁴Where only continuous transitions were taken into account.

⁵The introduced $1/L$ scaling of λ is to ensure that the CGF μ has the same system size scaling as the LDF.

as a minimization problem

$$\mu(\lambda) = \frac{L}{t} \inf_{\rho, p} \int dx d\tau s(x, \tau), \quad (3.9)$$

with ⁶

$$s(x, \tau) = p \partial_\tau \rho - \mathcal{H} \quad (3.10)$$

and

$$\mathcal{H} = D \partial_x \rho \partial_x p - \frac{1}{2} \sigma (\partial_x p)^2 \quad (3.11)$$

with the boundary conditions

$$\begin{cases} \rho(x=0, \tau) = \rho_l & \rho(x=1, \tau) = \rho_r \\ p(x=0, \tau) = 0 & p(x=1, \tau) = -\lambda. \end{cases} \quad (3.12)$$

Here, the minimization with respect to ρ and p gives Hamilton like equations,

$$\begin{cases} \partial_\tau \rho = \frac{\delta \mathcal{H}}{\delta p} \\ \partial_\tau p = -\frac{\delta \mathcal{H}}{\delta \rho}, \end{cases} \quad (3.13)$$

with $\frac{\delta \mathcal{H}}{\delta p} = \partial_x (D \partial_x \rho - \sigma \partial_x p)$ and $-\frac{\delta \mathcal{H}}{\delta \rho} = -D \partial_{xx} p - \frac{1}{2} \sigma' (\partial_x p)^2$. Later, it will prove useful to notice that the first equation in (3.13) is the continuity equation in disguise. Under the AP, the Hamilton equations become

$$\begin{cases} 0 = \partial_x (D \partial_x \rho - \sigma \partial_x p) \\ 0 = -D \partial_{xx} p - \frac{1}{2} \sigma' (\partial_x p)^2. \end{cases} \quad (3.14)$$

So far, it seems that using the CGF formalism simply reformulates the problem, since instead of solving the Euler-Lagrange equation (3.5), we need to solve (3.14). Indeed, solving either (3.5) or (3.14) is of the same order of difficulty. However, retrying the small perturbation approach described in (3.7), produces useful results.

3.3 Stability of Hamiltonian Systems

Consider an action-like expression

$$S(\rho, p) = \int dx d\tau s(x, \tau), \quad (3.15)$$

with $s(x, \tau)$ of the form (3.10), for some \mathcal{H} , an explicit function of (ρ, p) . The minimization of S with respect to ρ and p gives the (possibly time-dependent) Hamilton equations

$$\begin{cases} \partial_\tau \rho = \frac{\delta \mathcal{H}}{\delta p} \\ \partial_\tau p = -\frac{\delta \mathcal{H}}{\delta \rho}. \end{cases} \quad (3.16)$$

⁶There is an extra term $\int dx d\tau \lambda x \partial_\tau \rho$ in the CGF, however for current fluctuations and in the long time limit, this term is negligible, provided particle do not accumulate in the system.

Any $(\bar{\rho}, \bar{p})$ satisfying the Hamilton equations (3.16), are only guaranteed to be an extremal solution. To ensure a minimal solution, we require the convexity of S for any small perturbation $(\delta\rho, \delta p)$ around the extremal solution $(\bar{\rho}, \bar{p})$, namely,

$$S(\rho + \delta\rho, p + \delta p) + S(\rho - \delta\rho, p - \delta p) - 2S(\rho, p) > 0.$$

Hereafter, we evaluate the derivatives of \mathcal{H} at the extremal solution $(\bar{\rho}, \bar{p})$. For small fluctuations, we require $\delta S^2 > 0$ for the stability of the extremal solution, where⁷

$$\delta S^2 = \frac{1}{2} \int dx d\tau \left(\frac{\delta^2 \mathcal{H}}{\delta p^2} \delta p^2 + \frac{\delta^2 \mathcal{H}}{\delta \rho^2} \delta \rho^2 + 2 \frac{\delta^2 \mathcal{H}}{\delta \rho \delta p} \delta \rho \delta p - 2 \delta p \partial_\tau \delta q \right). \quad (3.17)$$

It is important to note that the first equation of (3.16) is the continuity equation in disguise, namely $\frac{\delta \mathcal{H}}{\delta p} = -\partial_x j$. This implies that the perturbations $(\delta\rho, \delta p)$ are not independent⁸. Linearizing the continuity equation around the extremal solution $(\bar{\rho}, \bar{p})$ gives

$$\partial_\tau \delta q = \frac{\delta^2 \mathcal{H}}{\delta p^2} \delta p + \frac{\delta^2 \mathcal{H}}{\delta p \delta \rho} \delta \rho + \mathcal{O}(\delta \rho^2, \delta p^2, \delta \rho \delta p). \quad (3.18)$$

Inserting (3.18) in (3.17) gives to second order

$$\delta S^2 = \frac{1}{2} \int dx d\tau \left(\frac{\delta^2 \mathcal{H}}{\delta \rho^2} \delta \rho^2 - \frac{\delta^2 \mathcal{H}}{\delta p^2} \delta p^2 \right). \quad (3.19)$$

We stress again that $(\delta q, \delta p)$ are coupled. In order to obtain their explicit expressions one must solve the set of linearized equations

$$\begin{aligned} \partial_\tau \delta q &= \frac{\delta^2 \mathcal{H}}{\delta p^2} \delta p + \frac{\delta^2 \mathcal{H}}{\delta p \delta \rho} \delta \rho, \\ \partial_\tau \delta p &= -\frac{\delta^2 \mathcal{H}}{\delta \rho^2} \delta \rho - \frac{\delta^2 \mathcal{H}}{\delta p \delta \rho} \delta p \end{aligned} \quad (3.20)$$

stemming from (3.16). For S to be convex around the $(\bar{\rho}, \bar{p})$, we require $\delta S^2 \geq 0$ for all the possible fluctuations that satisfy (3.20). Therefore, a sufficient condition for the stability of the solution $(\bar{\rho}, \bar{p})$ is for the integrand of (3.19) to be positive, namely

$\frac{\delta^2 \mathcal{H}}{\delta \rho^2} \geq 0$ and $\frac{\delta^2 \mathcal{H}}{\delta p^2} \leq 0$. It is not a sufficient and necessary condition as $\delta\rho$ and δp are coupled through (3.20).

In the case where the extremal solution is time-independent, we consider the Fourier spectrum of the time-dependent fluctuations $\delta\rho(x, \tau)$ and $\delta p(x, \tau)$ to find a necessary and sufficient condition for the stability of the solution. Since time is defined on $[0, t/L^2]$, the Fourier series expansions read $\delta\rho =$

⁷Here, all the derivatives and any other expression is to be understood as being evaluated at the extremal solution $(\bar{\rho}, \bar{p})$.

⁸As to be expected from the Lagrangian formalism where the density ρ and current j are coupled.

$\sum_{\omega} e^{i\omega\tau} f_{\omega}(x)$ and $\delta p = \sum_{\omega} e^{i\omega\tau} g_{\omega}(x)$, with the discrete frequencies $\omega_m = \frac{2\pi}{t/L^2} m$, for $m \in \mathbb{Z}$. The linearized equations (3.20) become

$$\begin{aligned} i\omega f_{\omega} &= \mathcal{H}_{pp} g_{\omega} + \mathcal{H}_{p\rho} f_{\omega}, \\ i\omega g_{\omega} &= -\mathcal{H}_{\rho\rho} f_{\omega} - \mathcal{H}_{p\rho} g_{\omega}, \end{aligned} \quad (3.21)$$

with⁹

$$\begin{aligned} \mathcal{H}_{pp} &= \frac{\delta^2 \mathcal{H}}{\delta p^2}, \\ \mathcal{H}_{\rho\rho} &= \frac{\delta^2 \mathcal{H}}{\delta \rho^2}, \quad \mathcal{H}_{p\rho} = \frac{\delta^2 \mathcal{H}}{\delta p \delta \rho}. \end{aligned}$$

One can rewrite (3.21) as a linear eigenvalue problem,

$$\bar{\mathcal{H}} v = i\omega \hat{v}, \quad (3.22)$$

for $\hat{v} = \begin{pmatrix} f_{\omega} \\ g_{\omega} \end{pmatrix}$ and $\bar{\mathcal{H}}(\bar{\rho}, \bar{p}) = \begin{pmatrix} \mathcal{H}_{pp} & \mathcal{H}_{p\rho} \\ -\mathcal{H}_{\rho\rho} & -\mathcal{H}_{p\rho} \end{pmatrix}$. Using the equalities $\int d\tau \delta q^2 = \sum_{\omega>0} |f_{\omega}|^2$ and $\int d\tau \delta p^2 = \sum_{\omega>0} |g_{\omega}|^2$, allows to rewrite (3.19) as $\delta S^2 = \sum_{\omega>0} \delta s_{\omega}^2$, with

$$\delta s_{\omega}^2 = \frac{1}{2} \int dx \left(\frac{\delta^2 \mathcal{H}}{\delta \rho^2} |f_{\omega}|^2 - \frac{\delta^2 \mathcal{H}}{\delta p^2} |g_{\omega}|^2 \right). \quad (3.23)$$

Now, we can formulate a sufficient and necessary condition for the convexity of S . S is convex about the extremal solution $(\bar{\rho}, \bar{p})$ if and only if $\delta s_{\omega}^2 \geq 0$ for any solution (f_{ω}, g_{ω}) of (3.21) and $\forall \omega > 0$.

Proof: Let us assume that $\delta s_{\omega}^2 \geq 0$ for any solution (f_{ω}, g_{ω}) of (3.21) and $\forall \omega > 0$. Then, necessarily, $\delta S^2 \geq 0$ for any fluctuation $(\delta\rho, \delta p)$ that satisfies (3.20) and $(\bar{\rho}, \bar{p})$ is a minimal solution. Conversely, if there exists a mode ω_0 , such that for the solution $(f_{\omega_0}, g_{\omega_0})$ of (3.21) $\delta s_{\omega_0}^2 < 0$, then, one can choose $\delta\rho = e^{i\omega_0\tau} f_{\omega_0} + e^{-i\omega_0\tau} f_{\omega_0}^*$ and $\delta p = e^{i\omega_0\tau} g_{\omega_0} + e^{-i\omega_0\tau} g_{\omega_0}^*$ so that $\delta s_{\omega}^2 = 0$ for any $\omega \neq \omega_0$. Therefore, this fluctuation leads to a value of the action lower than the extremal $(\bar{\rho}, \bar{p})$ solution, though not necessarily a new minimum.

3.4 Validity of the Additivity Principle

The general stability conditions derived in the previous section provide the theoretical framework needed to understand the validity of the AP. In the case of the MFT, \mathcal{H} is given by (3.11). So, the quadratic diagonal form (3.19) is $\delta S^2 = \frac{1}{2} \int dx d\tau \delta s_{AP}^2$, with^{10,11},

$$\delta s_{AP}^2 = \frac{D'_0 \sigma'_0 - D_0 \sigma''_0}{2D_0} (\partial_x \bar{p})^2 \delta \rho^2 + \sigma_0 (\partial_x \delta p)^2. \quad (3.24)$$

⁹Notice that $\mathcal{H}_{pp}, \mathcal{H}_{p\rho}, \mathcal{H}_{\rho\rho}$ are evaluated at $(\bar{\rho}, \bar{p})$ and are differential operators, which may in principle include spatial derivatives or non-linear functions of $\bar{\rho}, \bar{p}$.

¹⁰the zero subscript denotes evaluation at the AP solution $D_0 = D(\bar{\rho})$.

¹¹Notice that now the variation of the action with respect to δp , has to be written with $\partial_x \delta p$.

It is then straight forward to see that a sufficient condition for the validity of the AP becomes

$$D'_0\sigma'_0 \geq D_0\sigma''_0. \quad (3.25)$$

A similar condition was found in [37], where it was shown that $D'\sigma' \geq D\sigma''$ for any density profile is a sufficient condition for the validity of the AP. The sufficient condition (3.25) is less stringent than the one derived in [37], as it allows to verify the validity of the AP for a specific boundary conditions $\rho_{l,r}$ and for some value of λ . For a more detailed discussion, see the appendix of [38].

The sufficient and necessary condition for the validity of the AP, expressed in (3.21) and (3.23) translates here to requiring $\delta s_\omega^2 \geq 0$ for any solution (f_ω, g_ω) of

$$\begin{aligned} i\omega f_\omega &= \partial_x (D'_0\partial_x\bar{\rho}f_\omega + D_0\partial_x f_\omega - \sigma'_0\partial_x\bar{\rho}f_\omega - \sigma_0\partial_x g_\omega) \\ i\omega g_\omega &= \left(-D'_0\partial_{xx}\bar{\rho} - \frac{1}{2}\sigma''_0(\partial_x\bar{\rho})^2\right) f_\omega - D_0\partial_{xx}g_\omega - \sigma'_0\partial_x\bar{\rho}\partial_x g_\omega, \end{aligned} \quad (3.26)$$

with the boundary conditions

$$f_\omega(x=0,1) = g_\omega(x=0,1) = 0, \quad (3.27)$$

as the new fluctuation must satisfy the original boundary conditions and with

$$\delta s_\omega^2 = \int dx \left(\frac{D'_0\sigma'_0 - D_0\sigma''_0}{2D_0} (\partial_x\bar{\rho})^2 |f_\omega|^2 + \sigma_0 |\partial_x g_\omega|^2 \right). \quad (3.28)$$

It is to be understood that explicitly solving (3.26) and (3.28) is difficult. However, one can express (3.26) as a coupled linear ordinary differential equation which makes it numerically valuable. Therefore, the sufficient and necessary condition provides a useful numerical tool to prove the validity of the AP for specific boundary conditions and specific currents (in terms of the conjugate λ values).

3.4.1 The validity of the additivity principle for systems under a weak applied field

Considering now applying on the system a weak field E . One can show that \mathcal{H} becomes

$$\mathcal{H}_E = -D\partial_x\rho\partial_x p - \frac{1}{2}\sigma \left[(\partial_x p)^2 + 2E\partial_x p \right],$$

so that the AP Hamilton equations (3.14) rewrite

$$\begin{cases} 0 = \partial_x (D\partial_x\rho - \sigma [\partial_x p + E]) \\ 0 = -D\partial_{xx}p - \frac{1}{2}\sigma' \left[(\partial_x p)^2 + 2E\partial_x p \right]. \end{cases} \quad (3.29)$$

One can then show that

$$\delta s_\omega^2 = \int dx \left(\frac{D'_0\sigma'_0 - D_0\sigma''_0}{2D_0} \left[(\partial_x\bar{\rho})^2 + 2E\partial_x\bar{\rho} \right] |f_\omega|^2 + \sigma_0 |\partial_x g_\omega|^2 \right).$$

In principle, one can reproduce the previous approach for that case in order to obtain a reformulation of the sufficient and necessary criterion for boundary driven systems with an applied field E . We notice that the generalization to the sufficient condition seems non trivial, as we need to also require that $(\partial_x \bar{\rho})^2 + 2E\partial_x \bar{\rho} \geq 0$. However, it turns out that in the case of constant E , it is possible to show that indeed $(\partial_x \bar{\rho})^2 + 2E\partial_x \bar{\rho} \geq 0$ for any E through an implicit solution of (3.29). Defining $u = \partial_x \bar{\rho} + E$ allows to write the second equation of (3.29) under the form

$$\frac{du}{u^2 - E^2} = -\frac{\sigma'_0}{2D_0} dx. \quad (3.30)$$

Next, we define $h(x) \equiv -\int dx \frac{\sigma'_0}{2D_0}$, for a known density profile $\bar{\rho}$. An integral of (3.30) is implicitly obtained in terms of $h(x)$ under the form $u = E \coth(Eh(x))$. Therefore, $(\partial_x \bar{\rho})^2 + 2E\partial_x \bar{\rho} = E^2 / \sinh^2(Eh(x)) > 0$ for any E and (3.25) remains a sufficient condition for the validity of the AP for any E .

In what follows, we present two straightforward applications of the sufficient condition (3.25) and the sufficient and necessary condition expressed through (3.26) and (3.28).

3.5 Applications

3.5.1 The Weakly Asymmetric Exclusion Process

The first immediate application is for the weakly asymmetric exclusion process (WASEP). To define the WASEP, we consider a lattice gas, where each site can be occupied by no more than one particle. Particles can hop to empty neighboring sites with rates $1 \pm E/2L$, where the plus sign is for a right hand side jump and the minus for a left hand side jump¹² and with L the number of lattice sites. Macroscopically, we have $D = 1$ and $\sigma(\rho) = 2\rho(1 - \rho)$ [39]. For $E = 0$, the process is known as the simple symmetric exclusion process (SSEP). The sufficient condition (3.25) immediately shows that the AP is valid for the WASEP, as well as for the SSEP. While the SSEP is a well known example for a process that satisfies the AP [20, 37, 40], the validity of the AP in the WASEP was explored only numerically [27].

It is interesting to note that the WASEP was found to break the AP for some particular values of E in the case of periodic boundary conditions [34, 33]. We will revisit this point soon enough.

3.5.2 The KMP Process

Another model of interest is the KMP process¹³ [8]. It is a heat transfer model between two thermal baths (instead of particle reservoirs), where one can explicitly prove Fourier's law. This process does not correspond to the lattice

¹²This of course defines the WASEP for a $1d$ case.

¹³after Kipnis, Marchioro and Presutti.

gas picture presented in Chapter 2. However, it turns out that a macroscopic description is possible with $D = 1$ and $\sigma = 2\rho^2$, where the temperatures of the thermal baths is given by $\rho_{l,r} \in [0, \infty)$. A simple calculation shows that the sufficient condition (3.25) is not satisfied. Therefore, we must explore the sufficient and necessary condition numerically. To do that, one needs to solve (3.14) to obtain the AP solution in the CGF formalism. Secondly, one needs to solve (3.26). Numerically, it is advantageous to bring (3.26) to the form of two coupled differential equations, namely

$$\begin{aligned} \partial_{xx} f_\omega &= A_f f_\omega + B_f \partial_x f_\omega - i\omega \frac{\sigma_0}{D_0^2} g_\omega + C_f \partial_x g_\omega \\ \partial_{xx} g_\omega &= \frac{\sigma'_0 D'_0 - D_0 \sigma''_0}{2D_0^2} (\partial_x \bar{\rho})^2 f_\omega - \frac{i\omega}{D_0} g_\omega - \frac{\sigma'}{D_0} \partial_x \bar{\rho} \partial_x g_\omega, \end{aligned} \quad (3.31)$$

with

$$\begin{cases} A_f = \frac{1}{D_0} i\omega + \left\{ \frac{D_0'^2 - D_0'' D_0}{D_0^2} \right\} (\partial_x \bar{\rho})^2 + \left\{ \frac{D_0 \sigma_0'' - D_0' \sigma_0'}{D_0^2} \right\} \partial_x \bar{\rho} \partial_x \bar{\rho} \\ \quad + \frac{1}{2D_0^3} \{ 2D_0' \sigma_0 \sigma_0' - D_0 \sigma_0'^2 - D_0 \sigma_0 \sigma_0'' \} (\partial_x \bar{\rho})^2 \\ B_f = \frac{1}{D_0} (\sigma_0' \partial_x \bar{\rho} - 2D_0' \partial_x \bar{\rho}) \\ C_f = \frac{\sigma_0}{D_0} \partial_x \bar{\rho} - \frac{\sigma_0 \sigma_0'}{D_0^2} \partial_x \bar{\rho}. \end{cases}$$

The linearity of (3.31) lead to degenerate solutions. Therefore, due to the boundary conditions (3.27), $f = g = 0$ is a trivial solution. In order to obtain a useful solution, we assume the existence of a non-trivial solution $(\tilde{f}_\omega, \tilde{g}_\omega)$. Due to the linearity of (3.31), there exists some $\gamma \in \mathbb{C}$ such that $(\bar{f}_\omega, \bar{g}_\omega) = (\gamma \tilde{f}_\omega, \gamma \tilde{g}_\omega)$ is also a solution of (3.31), and $(\bar{f}_\omega, \bar{g}_\omega)$ satisfy the boundary conditions

$$\begin{cases} \bar{f}_\omega(x=0) = 0 & \bar{f}_\omega(x=1) = 0 \\ \bar{g}_\omega(x=0) = 0 & \partial_x \bar{g}_\omega(x=0) = 1. \end{cases} \quad (3.32)$$

This change of boundary conditions, allows to numerically search for the solution $(\bar{f}_\omega, \bar{g}_\omega)$, avoiding the trivial solution. If $(\bar{f}_\omega, \bar{g}_\omega)$ satisfies $\bar{g}_\omega(x=1) = 0$, then it is also a solution to the boundary value problem $\bar{f}_\omega(x=0) = \bar{f}_\omega(x=1) = \bar{g}_\omega(x=0) = \bar{g}_\omega(x=1) = 0$. Conversely, if $\bar{g}_\omega(x=1) \neq 0$, then the trivial solution is the only solution.

Employing this numerical procedure, we find only trivial solutions for a large range of currents $J \in [-14, 30]$ for the boundary conditions $\rho_l = 1, \rho_r = 2$ ¹⁴ (see Figures 3.1, 3.2 and 3.3). The values $J(\lambda)$ are found using the relation $\partial_\lambda \mu(\lambda) = J$ derived from (3.8) with $\mu(\lambda)$ is evaluated at the AP solution. This implies that the AP is valid for any current for the KMP process. We stress that we are able to verify this for a noticeably larger range of currents than was previously obtained via a direct simulation [22, 23, 24, 26]. It is also noteworthy that for periodic boundary conditions, one finds a breaking of the AP at some current J , sufficiently far (but of the same order of magnitude) from the steady state [34, 31, 32]. Together with the example of the WASEP, it would seem to

¹⁴As well as for other boundary conditions

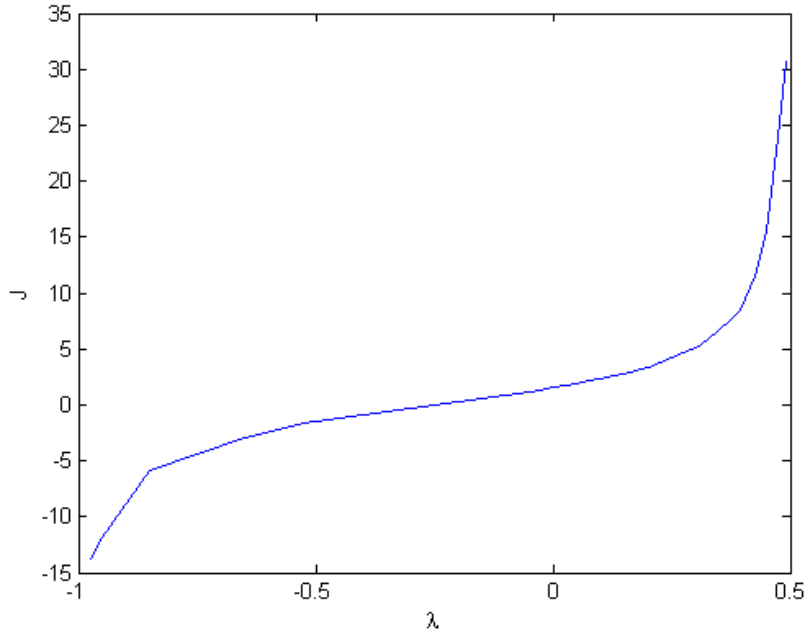


Figure 3.1: The λ to J conversion for the KMP model, with $\rho_l = 1, \rho_r = 2$.

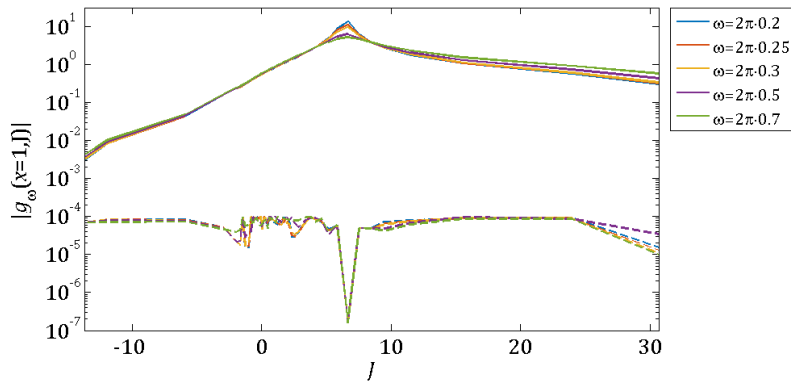


Figure 3.2: Stability analysis for the KMP model, with $\rho_l = 1, \rho_r = 2$. We show here $|g_\omega(x=1, J)|$ as a function of the current J for different values of ω . The full lines indicate $|g_\omega(x=1, J)|$ and the dashed lines, the estimated errors on evaluating g_ω . The values of $|g_\omega(x)|$ are decreasing to zero, but they never reach it as the numerical error is much too small.

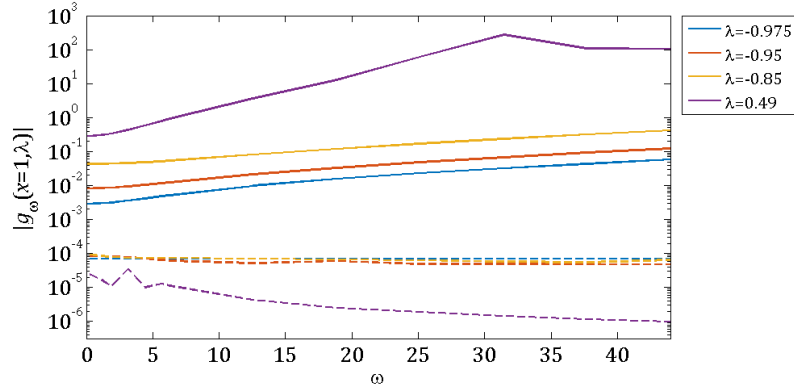


Figure 3.3: Stability analysis for the KMP model, with $\rho_l = 1, \rho_r = 2$. $|g_\omega(x=1)|$ is displayed as a function of the frequency ω for different values of λ . The full lines indicate $|g_\omega(x=1)|$ and the dashed lines, the estimated errors on evaluating g_ω . The values of $|g_\omega(x)|$ are decreasing to zero, but they never reach it as the numerical error is much too small.

suggest a trend where boundary driven processes are more AP stable than the same process on a ring geometry. We make this consideration more precise in the next section.

3.6 Remarks on dynamical phase transitions

So far, we have considered a continuous breaking of the AP solution. Namely, if there exists some critical value J_c , beyond which the AP is no longer valid, then the solution changes continuously at the breaking. This seems to correspond to a second order phase transition. One can also consider first order phase transitions, where at J_c , there are two (or more) different solutions to the minimization problem (3.3) with the first being the AP solution. Since (3.5) is a boundary value nonlinear differential equation, there is no guarantee for the existence of a unique solution. Therefore, it is possible that the second solution is also time-independent. Using the Hamiltonian formalism (3.6), this problem becomes equivalent to finding degenerate classical trajectories (in one spatial dimension) a classical particle takes from a point ρ_l to a point ρ_r at the normalized “time” $x \in [0, 1]$. An example for such degeneracies, was shown in [41], however the macroscopic model does not follow any microscopic physical picture. The present equivalence allows to give a physical meaning to such degeneracies.

Another possibility for a first order transition is to find, aside from the AP solution, a second time-dependent solution for the Hamilton equations (3.13). Such a time-dependent solution give rise to a transfer of Q particles between the reservoirs in an efficient way that competes with the AP solution. Quantitatively, the options are limited. One such mechanism is for the particles to

flow between the reservoirs in “big” bunches, at some velocity. The bunched are separated by a macroscopic distance¹⁵, which translates to a macroscopic time delay $\alpha \frac{t}{L^2}$ between the arrival of each bunch to a reservoir, where they are being depleted. We can also consider a mechanism where the particles bunch to a single group, that flows with some velocity between the reservoirs. Building up on one end and being depleted on the other.

Back to second order phase transitions. We recall that for the KMP process and the WASEP, a dynamical phase transition was found for a ring geometry (periodic boundary conditions), but not for boundary driven processes. We propose that this condition is rather general, and one can expect that boundary driven processes are more stable than processes on a ring. The mechanism found for these second order phase transitions [31, 34, 42, 37], is a traveling wave, carrying a bulk of particles, responsible for the current. Periodic systems generate this wave once, and then propagate it. For boundary driven systems, there is an additional cost in the LDF for such a traveling wave, since it is created and destroyed a number of times, scaling like t , at the boundaries. Therefore, this mechanism is less likely in boundary driven systems. Mathematically, this condition can be proven exactly for certain processes. For periodic systems, it was found that a necessary condition for the breaking of the AP is $\sigma'' > 0$. For a process with $\frac{D'\sigma'}{D} > \sigma'' > 0$, this implies a phase transition for a ring geometry. However, for a boundary driven process, the sufficient condition (3.25) is satisfied, and the process is stable. Moreover, even for $\frac{D'\sigma'}{D} - \sigma''$ not strictly positive, this does not imply a phase transition for the boundary driven process, since (3.25) is a sufficient condition only. Prominent examples for this are the KMP process which is unstable for periodic systems, but stable for boundary driven processes, as well as the WASEP.

¹⁵To be discernible in the MFT and different from the AP solution.

Chapter 4

Universal Current Fluctuations

Building on the stability of the AP assumption, we discuss in this chapter the universality of current fluctuations for arbitrary geometries. The CGF is found to be universal up to a scaling factor, depending only on the geometry of the system. This scaling factor is shown to be the effective capacitance of the system, just like in potential theory. In the last section, we provide numerical evidence for our claim for the SSEP. The analytical proof in Section 4.1 mostly follows [43].

4.1 Universality of the CGF

We are interested in finding the probability to observe Q_t particles flowing from reservoir A to reservoir B , after a long time t . Assuming that particles cannot accumulate in the system, we obtain that asymptotically $Q_t = Q_t^A = Q_t^B$ for $t \rightarrow \infty$, where Q_t^A (Q_t^B) are the number of particles that flowed from (to) the reservoir A (B) into (from) the system. For an arbitrary graph with vertices $i \in G$, coupled to two reservoirs $i = A, B$ at fixed densities ρ_a, ρ_b correspondingly, we define $q_{i,j}(t)$ to be the number of particles that flowed from site i to site j (if they share a link) after time t . Moreover, we introduce a potential like function V_i which is constraint at A, B to $V_A = 1$ and $V_B = 0$. Asymptotically for a large time t ,

$$Q_t = \frac{1}{2} \sum_{i,j} (V_i - V_j) q_{i,j}(t). \quad (4.1)$$

Using that $n_i(t) - n_i(0) = \sum_{i \sim j} q_{i,j}(t)$ ¹, with $n_i(t)$ being the number of particles at site i and time t , we rewrite (4.1) as

$$Q_t = \sum_i V_i \sum_{j \sim i} q_{i,j}(t) = V_A \sum_{j \sim A} q_{A,j}(t) + V_B \sum_{j \sim B} q_{B,j}(t) + \sum_{i \neq A,B} V_i (n_i(t) - n_i(0)). \quad (4.2)$$

We obtain that asymptotically, $Q_t = \sum_{j \sim A} q_{A,j}(t) = Q_t^A$, since we choose $V_A = 1, V_B = 0$ and the third term in (4.2) is bounded as the graph can only accommodate a finite number of particles, while Q_t, Q_t^A scale linearly in time. In what follows, we choose V to be the solution of the Laplace equation $\Delta V = 0$, with the boundary conditions $V_A = 1, V_B = 0$, which translates to $\Delta V_i = \sum_{j \sim i} V_j - V_i$.

Extending the MFT to d dimensions changes the fundamental formula (2.3) to

$$P_t(\{j, \rho\}) \sim \exp -L^d \int_0^1 d^d \mathbf{x} \int_0^{t/L^2} d\tau \mathcal{L}(\mathbf{j}, \rho), \quad (4.3)$$

with

$$Q_t = L^2 \int d\tau d^d \mathbf{x} \nabla v(\mathbf{x}) \cdot \mathbf{j}(\mathbf{x}, \tau),$$

as a continuous version of (4.1), where $v(\mathbf{x})$ is the continuous version of V_i . The CGF can be written as

$$\mu_G(\lambda) = \frac{L^d}{t} \inf_{\rho, p} \int d^d \mathbf{x} d\tau s(\mathbf{x}), \quad (4.4)$$

with

$$s(\mathbf{x}) = -D \nabla \rho \nabla p + \frac{1}{2} \sigma (\nabla p)^2,$$

where the boundary value of p is now $p(\mathbf{x} = B) = 0$ and $p(\mathbf{x} = A) = -\lambda$. The corresponding Hamilton equations under the AP are

$$\begin{cases} 0 = \nabla (D \nabla \rho - \sigma \nabla p) \\ 0 = -D \nabla^2 p + \frac{1}{2} \sigma (\nabla p)^2. \end{cases} \quad (4.5)$$

Consider now the AP solution to the corresponding one dimensional problem, $\bar{\rho}(x), \bar{p}(x)$. It is easy to check that $\bar{\rho}(v(\mathbf{x})), \bar{p}(v(\mathbf{x}))$ is the AP solution to (4.5) provided $\Delta v(\mathbf{x}) = 0$, for $V_A = 1, V_B = 0$. A similar idea was used in [2]. Using this solution in (4.4), we find that

$$\mu_G(\lambda) = L^{d-2} \int d^d \mathbf{x} (\nabla v(\mathbf{x}))^2 \left(-D (\bar{\rho}) \nabla \bar{\rho} \nabla \bar{p} + \frac{1}{2} \sigma (\bar{\rho}) (\nabla \bar{p})^2 \right). \quad (4.6)$$

A useful integral identity shows that

$$\int d\mathbf{x} v(\mathbf{x})^n (\nabla v)^2 = \frac{1}{n+1} \int d\mathbf{x} (\nabla v)^2 = \int_0^1 dx x^n \times \int d\mathbf{x} (\nabla v(\mathbf{x}))^2.$$

¹ $i \sim j$ denotes summing over all the neighbors j of i .

Therefore for any smooth function $\tilde{s}(x)$, we find

$$\int d^d \mathbf{x} \tilde{s}(v(\mathbf{x})) (\nabla v(\mathbf{x}))^2 = \int_0^1 dx \tilde{s}(x) \times \int d^d \mathbf{x} (\nabla v(\mathbf{x}))^2, \quad (4.7)$$

where we assumed \tilde{s} can be written as a polynomial series in x . Using (4.7) for (4.6), we find

$$\mu_G(\lambda) = C_{\text{eff}} \times \mu_1(\lambda), \quad (4.8)$$

where

$$\mu_1(\lambda) = \int_0^1 dx \left(-D(\bar{\rho}(x)) \partial_x \bar{\rho}(x) \partial_x \bar{p}(x) + \frac{1}{2} \sigma(\bar{\rho}(x)) (\partial_x \bar{p}(x))^2 \right)$$

is the solution to the one dimensional problem and $C_{\text{eff}} = \int d^d \mathbf{x} (\nabla v(\mathbf{x}))^2$ is a geometrical factor, independent on the system dynamics D, σ or on the values of λ, ρ_a, ρ_b . It is tempting to understand (4.8) and particularly C_{eff} in terms of potential theory and of effective capacitance for the system. This is the content of the next section.

4.2 Energy Forms

For a network of capacitors, coupled to a voltage drop δV , it is well known that one can replace the entire network by a single effective capacitor. One way to find the value of the effective capacitance of the system, is by using energy forms. We consider the same graph G as before, where at each bond connecting vertices x and y , lies a capacitor c_{xy} . The energy of the bond is given by $\frac{1}{2} c_{xy} (V(x) - V(y))^2$. Therefore, one may write the energy of the network as a minimization problem

$$E_G = \min_V \frac{1}{2} \sum_{x \sim y} c_{xy} (V(x) - V(y))^2,$$

where V is constrained only at the boundaries A, B . Simple dimensional analysis shows that $E_G = \frac{1}{2} C_{\text{eff}} (\delta V)^2$, where C_{eff} is a function of all the $\{c_{xy}\}_{x \sim y}$. Therefore, C_{eff} here turns out to be the effective capacitance of the capacitors system. Setting all the $c_{xy} = 1$, $\delta V = 1$, allows to recast the minimization problem of E_G , as the Laplace equation $\Delta V = \sum_{x \sim y} V(x) - V(y) = 0$, with the boundary conditions $V_A = 1, V_B = 0$. We thus obtain that² $E_G = \frac{1}{2} C_{\text{eff}} \delta V^2 = \frac{1}{2} \sum_{x \sim y} (V(x) - V(y))^2$. The continuous version amounts to solving the Laplace equation $\Delta v(\mathbf{x}) = 0$, with $E_G / \frac{1}{2} \delta V^2 = L^{d-2} \int d^d \mathbf{x} (\nabla v(\mathbf{x}))^2 = C_{\text{eff}}$. Therefore, C_{eff} is the effective capacitance of the system.

For the MFT, the capacitance is basically the inverse of the effective system size $C_{\text{eff}} = 1/L^*$ for a $1d$ system. Due to the similarity with potential theory, we expect the Kirchhoff laws to apply as a method to find the effective conductance.

²Where the $\frac{1}{2}$ factor is due to double counting.

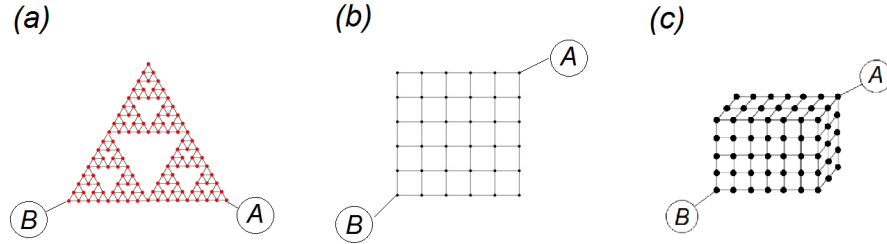


Figure 4.1: The graphs of the first group. (a) the Sierpinski gasket (b) the square lattice (c) the cubic lattice. All the graphs are coupled to the reservoirs A and B through a single bond. A bond indicates that a particle can hop between the vertices with rate 1. Vertices indicate sites.

Connecting systems in series and in parallel was already shown to follow the usual Kirchhoff rules of adding capacitors in series and parallel in [20]. Here it was shown for the first time that the analogy is exact. As a last remark, let us stress that C_{eff} follows Kirchhoff laws only if the system is coupled to each reservoir through a single bond. If this is not the case, potential theory still gives the correct results. While Kirchhoff rules are generally not satisfied, we can expect that for large enough systems, they still hold if the connection of the system to the reservoirs is through a finite (and small) number of bonds. In the next section, we present numerical data supporting our claims as well as a discussion on the finite size corrections to the hydrodynamically exact result and some possible generalizations.

4.3 Numerical Results

In this section, we provide numerical evidence for the universality of currents for the SSEP using the method explained in appendix A. We present the results for a few distinct geometries. We also discuss finite size corrections and possible generalizations.

We present the first few cumulants of the current fluctuations for two groups of graphs.

1. The Sierpinski gasket, a square lattice and a cubic lattice, depicted in Figure 4.1.
2. A set of three fractals known as diamond fractals, depicted in Figure 4.4.

Each reservoir is connected to the graph through one bond. The reservoir densities are set to be source & drain. Through the numerical method described in appendix A, the mean current I , the Fano factor F , defined as the ratio of the second and first cumulants, and the second Fano factor F_2 , defined as the ratio of the third and second cumulants, have been obtained. For the first group, according to Kirchhoff rules, we expect the effective number of sites L^* to go

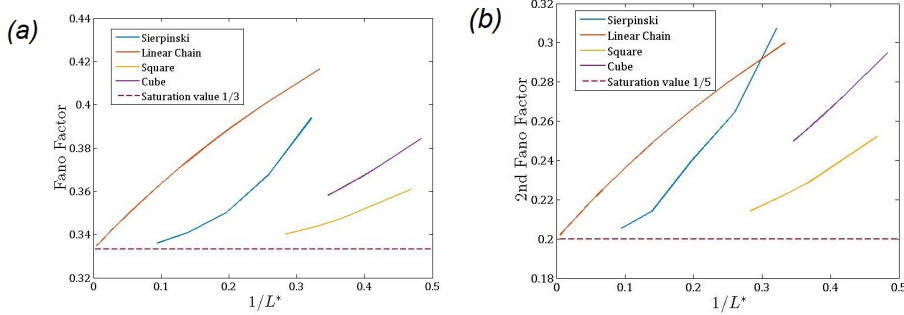


Figure 4.2: The convergence of the Fano factor F (a), and of the second Fano factor F_2 (b), are presented for the first group of geometries. F and F_2 are plotted versus the inverse effective number of sites for a finite graph and compared with exact results for the $1d$ (linear) chain. The plots indicate convergence to the expected values $F = 1/3$ and $F_2 = 1/5$.

to infinity. Comparing with the exact results for a $1d$ chain [40], we expect the Fano factor to converge to $1/3$ for (effective) small capacitance and the second Fano factor to converge to $1/5$ (see Figure 4.2). We expect that the finite size corrections for a finite system depends on the effective number of sites. The MFT cannot account for $1/L$ corrections and indeed for a $1d$ chain, the exact result corresponds to this $1/L$ correction [40]. For different geometries, nothing guarantees that the corrections will not be smaller, which is what we find (Figure 4.3). However, the scaling of the corrections are expected to be the same for the first and second Fano factor. For the range of values we were able to explore numerically, it seems to be indeed the case (Table 4.1). We therefore deduce that the finite size corrections are not universal, which is to be expected.

For the second group of graphs, Kirchhoff rules imply that $L^* \rightarrow \text{const.}$ So that F and F_2 do not converge to $1/3$ and to $1/5$. Therefore, it is difficult to ascertain any power law corrections, as L^* spans over a small region. The results for the convergence of F, F_2 of the second group are summarized on Table 4.2, where the simulation values are presented together with the expected values using Kirchhoff rules.

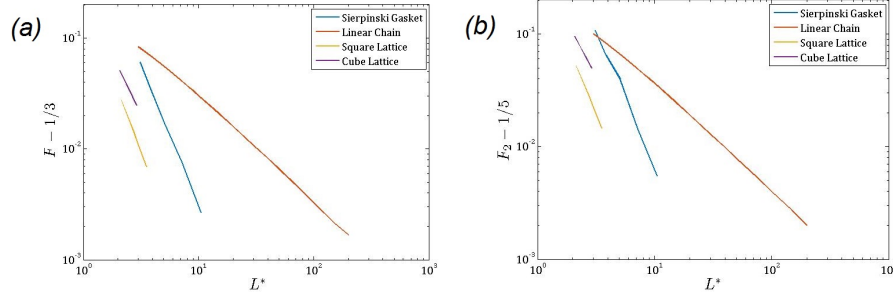


Figure 4.3: A log-log plot of the finite size corrections for the Fano factor F convergence to $1/3$ (a) and the second Fano factor F_2 to $1/5$ (b) versus the inverse of the effective system size are presented for the first group of geometries. For large effective system size, we find power law corrections $F = 1/3 + \mathcal{O}(L^{*\alpha})$ and $F = 1/3 + \mathcal{O}(L^{*\beta})$. As expected, α and β are not universal, however, they seem to satisfy $\alpha \approx \beta$ (see Table 4.1).

Table 4.1: Scaling exponents for the finite size corrections. The finite size corrections to the Fano factor F scale like $\sim L^{*\alpha}$, while for F_2 they scale like $\sim L^{*\beta}$, with L^* the effective number of sites expected from Kirchhoff resistor rules. From the MFT, one expects that for a linear chain $\alpha = \beta \leq -1$. Moreover, for any graph, one should expect $\alpha = \beta$ which seems to be supported by our findings, considering the low effective number of sites we are able to achieve numerically. The MFT cannot account for the value of α, β .

Graph	α	β
Linear chain	-0.9441	-0.9399
Sierpinski gasket	-2.5385	-2.4433
Square lattice	-2.7636	-2.5527
Cubic lattice	-2.1639	-1.9326

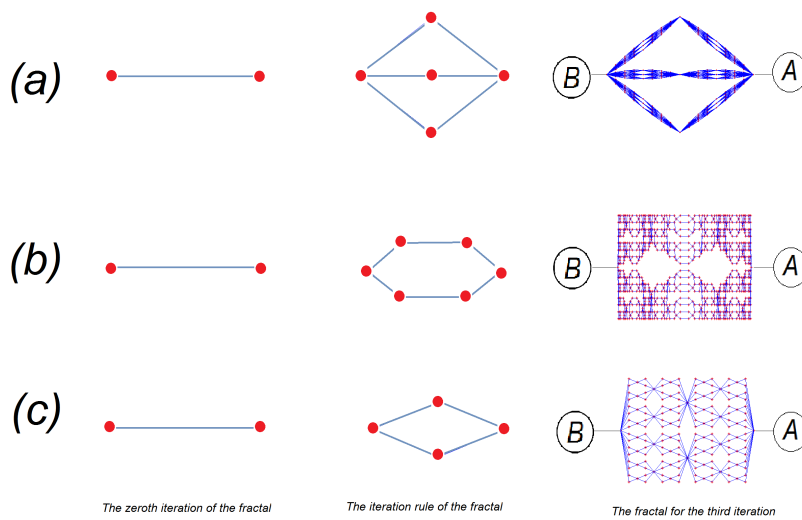


Figure 4.4: Graphs of the second group. Each line represents the iteration rule for the fractal (first to second column) and the full fractal appear in the third column for (a) Diamond $D_{6,3}$ fractal, (b) Diamond $D_{6,2}$ fractal and (c) Diamond $D_{4,2}$ fractal. All the graphs are coupled to the reservoirs A and B through a single bond.

Table 4.2: Cumulants of the SSEP on the second group graphs. (a) the diamond fractal $D_{6,2}$, (b) the diamond fractal $D_{6,2}$, (c) the diamond fractal $D_{4,2}$. The tables read as follows: n is the iteration level; I the current; $L^\# = 1/I$ is the numerically evaluated effective number of sites; L^* is the theoretical effective number of sites for Kirchhoff resistor rules, $F^\#$ is the numerically evaluated Fano factor; F^* is the theoretical prediction for the Fano factor from Kirchhoff rules.

The diamond fractal $D_{6,3}$ (a) in Figure 4.4.(a).

\hat{n}	\bar{I}	$L^\#$	L^*	$\bar{F}^\#$	\bar{F}^*
2	0.4091	2.4444	$2 + (2/3)^2 = 2.4444$	0.4256	0.4301
3	0.4355	2.2962	$2 + (2/3)^3 = 2.2963$	0.4436	0.4345

The diamond fractal $D_{6,2}$, (b) in Figure 4.4.(b).

\hat{n}	\bar{I}	$L^\#$	L^*	$\bar{F}^\#$	\bar{F}^*
2	0.2353	4.2499	$2 + (3/2)^2 = 4.25$	0.3573	0.3968
3	0.1860	5.3763	$2 + (3/2)^3 = 5.375$	0.3442	0.3856

The diamond fractal $D_{4,2}$ (c) in Figure 4.4.(c).

\hat{n}	\bar{I}	$L^\#$	L^*	$\bar{F}^\#$	\bar{F}^*
1	0.3333	3	3	0.3889	0.4167
2	0.3333	3	3	0.3845	0.4167
3	0.3333	3	3	0.3833	0.4167

In summary, we find an excellent agreement with the theoretical prediction given in (4.8). We have probed the finite size scaling for various graphs and have shown that there are non-universal as expected. We also understand the behavior of current fluctuations for systems coupled to more than two reservoirs through Kirchhoff rules, although the results are expected to converge more slowly [43].

Chapter 5

The MFT and Quantum Transport

The purpose of this chapter is to demonstrate how the MFT allows to study a wider class of processes than is currently considered. We use the results obtained in all previous chapter to argue that the MFT is an appropriate framework to study the noise and current statistics in disordered quantum mesoscopic conductors (at zero temperature), wave speckles [44, 45], non equilibrium spins in superconductors [46] and thermal transport [47, 48] to name a few. In the first section, we show how the Langevin equation at the basis of the MFT can be modified to address transport problems in disordered quantum processes or waves. In the second section, we discuss another relevant quantity; namely (out-of-equilibrium) density correlations. As density correlations are time-independent, their MFT description under the AP should be exact for mesoscopic systems. In the third section, we present two examples of a correspondence between classical and disordered quantum processes and we show that they lead to identical results, for current fluctuations and (out-of-equilibrium) density correlations. In the last part, we comment on future directions.

5.1 Langevin Approach to Mesoscopics

In Chapter 2, we discussed the Langevin approach to derive the MFT. Starting from (2.2), and for a white noise η allows to deduce the probability to observe a fluctuation. It is clear that (2.2) is a stochastic equation. While the microscopic evolution of the particles may be deterministic, it is often useful when dealing with many degrees of freedom to use a stochastic equation. Moreover, the source of stochasticity (thermal, quantum, disorder, etc.) is immaterial for any quantity derived from the Langevin equation. In the lattice gas case, one may consider that the system kept at a fixed, non-zero temperature. Then thermal fluctuations are the cause of the stochasticity.

It is tempting to try to use the Langevin approach to describe different

out of equilibrium systems, where the stochasticity does not arise from thermal fluctuations. Let us try and use these ideas to transport of quantum particles, flowing through a disordered medium at zero temperature. The current can be induced e.g. by a change of chemical potential, caused by a voltage drop. The disorder is accounted by quenched scatterers. At the simplest level, we consider the quantum particles to be non-interacting. Thus, their motion consists of a series of ballistic motion, occurring between elastic collision events. In the case of multiple scattering and for weak disorder, it is possible to write the propagation of the particle using a diffusion equation due to a diagrammatic expansion (see [44] for a full derivation). The resulting diffusion constant is $D = l_e v_e / d$, where v_e is the group velocity of the particle, d is the dimensionality of the system and l_e is the resulting transport mean free path. This description implies that a large system size $L \gg l_e$ is required to observe this diffusive behavior. One can therefore consider the classical Langevin equation (2.2) to govern the steady state fluctuations of the density profile and of the current. The conductivity σ can be obtained from the Kubo formula [44], where the diffusion coefficient D and the conductivity σ obtain all the relevant quantum information. This is in essence a semi-classical and coarse grained description of the system. Now, as the temperature is set to zero, the thermodynamic Einstein relation becomes [44, 49]

$$\sigma/D = e^2 \nu, \quad (5.1)$$

with ν being the density of states and e is the “charge” of the quantum particle.

Obtaining D and σ , one deduce the Langevin equation. In what follows, we consider quenched scatterers,

$$\begin{cases} \overline{\eta(x, \tau)} = 0 \\ \overline{\eta(x, \tau) \eta(x', \tau')} = \frac{1}{L} \delta(x - x'), \end{cases} \quad (5.2)$$

where the averaging $\overline{}$ is with respect to the realizations of disorder. The probability to observe a density and current fluctuation is¹

$$P_t(\{j(x), \rho(x)\}) \sim \exp - \frac{t}{L} \int_0^1 dx \mathcal{L}(j, \rho) \quad (5.3)$$

with

$$\mathcal{L}(j, \rho) = \frac{(j(x) + D(\rho(x)) \partial_x \rho(x))^2}{2\sigma(\rho(x))}.$$

The purpose of the rest of this Chapter is to present a correspondence between such disordered quantum processes to classical processes. This analogy is for processes with identical D and σ ². However, for the classical processes we have considered so far, time dependence was allowed. Therefore, the correspondence holds only for quantities where the time dependence does not explicitly manifest

¹For the sake of simplicity, we address the diffusion and the conductivity as dimensionless quantities.

²Up to irrelevant pre-factors.

itself such as current fluctuations, where the AP holds. Another quantity is the (out of equilibrium) density correlations function [30, 12, 1]. In the next section, we shortly summarize how to obtain the density correlations within the MFT formalism.

5.2 Density Correlations

For out of equilibrium systems, one generically finds long range correlations [50, 51]. Fortunately, the MFT allows to obtain analytic expressions for different processes characterized by D and σ . In this discussion, we follow ideas presented in [12]. We consider $1d$ systems for simplicity, however, the forthcoming results can be generalized to all dimensions. We define correlations functions by

$$C_n(x_1, x_2, \dots, x_n) = \langle \rho(x_1) \rho(x_2) \dots \rho(x_n) \rangle. \quad (5.4)$$

To evaluate C_n , it is useful to consider first the large deviation functional $\mathcal{F}(\hat{\rho}(x))$,

$$\exp[-L\mathcal{F}(\hat{\rho}(x))] = \min_{j, \rho} \int \mathcal{D}j \mathcal{D}\rho e^{-L \int dx d\tau \mathcal{L}(j, \rho)} \delta(\rho(x, \tau = t/L^2) - \hat{\rho}(x)), \quad (5.5)$$

which evaluates the probability to observe a density fluctuation $\hat{\rho}(x)$ at some long time t starting from the steady state density profile at a given initial time³. Using the more convenient Hamiltonian form, leads to

$$\exp[-L\mathcal{F}(\hat{\rho}(x))] = \min_{\rho, p} \int \mathcal{D}p \mathcal{D}\rho e^{-L \int dx d\tau p \partial_\tau \rho - \mathcal{H}(j, \rho)}, \quad (5.6)$$

where we have suppressed the constraint $\rho(x, \tau = t/L^2) = \hat{\rho}(x)$. A simple use of analytical mechanics (see [5, 6, 52]), shows that

$$\int dx \mathcal{H}\left(\rho, \frac{\delta \mathcal{F}}{\delta \rho}\right) = 0. \quad (5.7)$$

It is also useful to define a pressure functional,

$$\mathcal{G}(h) = \max_{\hat{\rho}} \left\{ \int dx [h(x) \hat{\rho}(x)] - \mathcal{F}(\hat{\rho}(x)) \right\}. \quad (5.8)$$

By Legendre duality, we identify $h = \frac{\delta \mathcal{F}}{\delta \hat{\rho}}$ and $\hat{\rho} = \frac{\delta \mathcal{G}}{\delta h}$, so that (5.7) implies

$$\int dx \left[\frac{1}{2} \sigma \left(\frac{\delta \mathcal{G}}{\delta h} \right) (\partial_x h)^2 - \partial_x h D \left(\frac{\delta \mathcal{G}}{\delta h} \right) \partial_x \frac{\delta \mathcal{G}}{\delta h} \right] = 0, \quad (5.9)$$

recalling that h vanishes at the boundaries. The pressure functional $\mathcal{G}(h)$, is a generating function, namely

$$C_n = \frac{\delta^n \mathcal{G}(h)}{\delta h(x_1) \delta h(x_1) \dots \delta h(x_n)} \Big|_{h=0}.$$

³When we consider $t \rightarrow \infty$, it should be clear that this initial time is not relevant.

Since \mathcal{F} has a minimum for ρ_s the steady state density profile, one can expand \mathcal{G} to second order in h ,

$$\mathcal{G}(h) = \int dy h(y) \rho_s(y) + \frac{1}{2} \int dy C_2(x, y) h(x) h(y) + \mathcal{O}(h^2).$$

Expanding also (5.9) up to second order in h , we obtain

$$\int dx \partial_x h \left[\frac{1}{2} \sigma(\rho_s) (\partial_x h) - \partial_x \left[\frac{1}{2} D(\rho_s) \int dy C_2(x, y) h(y) \right] \right] = 0. \quad (5.10)$$

Therefore, defining

$$C_2(x, y) = C_{eq}(x) \delta(x - y) + B(x, y) \quad (5.11)$$

where

$$C_{eq}(x) = D^{-1}(\rho_s(x)) \sigma(\rho_s(x)) \quad (5.12)$$

defines the equilibrium correlations for the steady state density profile $\rho_s(x)$, and $B(x, y)$ defines the out-of-equilibrium correlations. Setting (5.11) in (5.10), and using integration by parts, one can show that $B(x, y)$ satisfies

$$\mathcal{R}^\dagger B(x, y) = a(x) \delta(x - y), \quad (5.13)$$

where \mathcal{R}^\dagger is the formal adjoint of $\mathcal{R} = \mathcal{R}_x + \mathcal{R}_y$ ⁴ with

$$\begin{cases} \mathcal{R}_x = D(\rho_s(x)) \partial_{xx} \\ \mathcal{R}_y = D(\rho_s(y)) \partial_{yy} \end{cases}$$

and

$$a(x) = -\partial_{xx} [\sigma(\rho_s(x))].$$

In the case of quadratic σ and constant D as for the KMP or the SSEP, we obtain

$$B(x, y) = -\frac{\sigma''}{2D} (\partial_x \rho_s) \Delta^{-1}(x, y), \quad (5.14)$$

where $\Delta^{-1}(x, y)$ is the Green's function of the Dirichlet Laplacian; namely $(\partial_{xx} + \partial_{yy}) \Delta^{-1}(x, y) = \delta(x, y)$.

The previous results can be generalized to the correlation function $C_2(\mathbf{x}, \mathbf{y})$ in d dimensions. We recover (5.11), with the equilibrium fluctuations (5.12). The long range term $B(\mathbf{x}, \mathbf{y})$ is still given by (5.13) with $x \rightarrow \mathbf{x}$

$$a(\mathbf{x}) = -\partial_{x_i} \left[\sigma_{ij}(\rho_s(\mathbf{x})) D_{jk}^{-1}(\rho_s(\mathbf{x})) D_{kl}(\rho_s(\mathbf{x})) \partial_l \rho_s(\mathbf{x}) \right]$$

with i, j, k, l running over the spatial directions and \mathcal{R}^\dagger is the formal adjoint of $\mathcal{R} = \mathcal{R}_\mathbf{x} + \mathcal{R}_\mathbf{y}$ with

$$\mathcal{R}_\mathbf{x} = D_{ij}(\rho_s(\mathbf{x})) \partial_{x_i} \partial_{x_j}.$$

In the following section, we consider two examples in mesoscopic physics, where application of the MFT formalism reproduces known and new results.

⁴We choose to symmetrize \mathcal{R} . One can also take $\mathcal{R} = 2\mathcal{R}_x$ to obtain similar results.

5.3 Applications

5.3.1 Intensity Fluctuations of Coherent Light and the KMP

In this section, following [45], we wish to study the mesoscopic fluctuations of the optical transparency of dielectric media which scatter light elastically. The intensity of the scattered light from an incident coherent light beam fluctuates as a result of the location of the scatterers. The interference pattern resulting from the scattering is known as a speckle. We are interested to develop a theory that accounts for intensity fluctuations in the case of many scattering events in the medium due to different disorder realizations in the medium. In this context, $\bar{\mathcal{O}}$ denotes averaging with respect to the different disorder realizations.

We consider the regime $\lambda \ll l_e \ll L$, where λ is the wavelength of the light, l_e is the mean free path between scattering events and L is the system size. We assume that the absorption length and the coherence length are much larger than the system size (no losses and coherent light). The intensity of light, averaged with respect to disorder realizations $I_d(\mathbf{r})$, follows a diffusion equation (see [44] Chapter 4.7)

$$-D\Delta I_d(\mathbf{r}) = \delta(\mathbf{r} - \mathbf{r}_0), \quad (5.15)$$

where \mathbf{r}_0 is the location the incident beam impinges on the scattering medium⁵. D is the diffusion coefficient, given by $D = \frac{l_e c}{d}$, with c the propagation velocity of light in the medium and d the dimensionality of the medium. We would like to write an equation for the fluctuations in the energy flux \mathbf{J} . The intensity is related to the energy density u by $I_d = cu$. The continuity equation for the energy density reads $\partial_t u = -\nabla \cdot \mathbf{J}$. Applying (5.15) for the continuity equation allows to obtain the steady state energy flux $\bar{\mathbf{J}} = -D\nabla \bar{u}$. The energy density $\bar{u}(\mathbf{r})$, and the energy flux $\bar{\mathbf{J}}$ are assumed to vary smoothly over distances of the scale of l_e . The fluctuations over small scales due the different disorder realizations can be considered through a Langevin approach in the form of extraneous fluxes $\mathbf{j}_{ext}(\mathbf{r})$, namely

$$\mathbf{J}(\mathbf{r}) = -D\nabla n(\mathbf{r}) + \mathbf{j}_{ext}(\mathbf{r}),$$

where the $\overline{\mathbf{j}_{ext}}(\mathbf{r}) = 0$ follows the steady state intensity flux. From a detailed microscopic calculation [45] the correlator of the random extraneous fluxes is given by $\overline{\mathbf{j}_{ext}(\mathbf{r})\mathbf{j}_{ext}(\mathbf{r}')} = \delta_{ij}\sigma(\bar{u})\delta(\mathbf{r} - \mathbf{r}')$ for $|\mathbf{r} - \mathbf{r}'| \gg l_e$, where i, j denote the spatial directions and $\sigma = \frac{2\pi}{3}l_e\lambda^2 c^2 \bar{u}^2$. The idea behind this Langevin formalism, is that the intensity fluxes and densities resulting from random interference of the waves scattered by the randomly distributed scatterers can be grouped to microscopic fluctuations for $|\mathbf{r} - \mathbf{r}'| < l_e$ and diffusive fluctuations for $|\mathbf{r} - \mathbf{r}'| > l_e$. From this approach, one can go on and obtain the spatial intensity correlations [45] which was our goal here.

This Langevin approach is no different than the one used to develop the MFT formalism. So, this coarse grained approach, introduced in [45], describes

⁵One can generalize this to any incident beam and not jut a point source.

the fluctuations of the intensity flux and density using the diffusion D and conductivity σ only. Moreover, we identify that the problem of intensity fluctuations of coherent light in disordered medium, corresponds in the language of the MFT to the KMP process. At the first level, it allows to obtain the spatial intensity correlations using the method presented in section (5.2). In [53], it was shown that the Langevin approach of [45] allows to write the intensity correlation function $C_2 = C_{short} + C_{long}$ corresponding to the short range correlations $|r - r'| \ll l_e$ and the long range correlations⁶. It was found that $C_{short} = D^{-1}\sigma(\bar{u}(\mathbf{r}))\delta_{ij}\delta(\mathbf{r} - \mathbf{r}')$ which exactly matches to the equilibrium correlations C_{eq} in the language of the MFT. The long range correlations are indeed described by the result obtained in (5.14).

Considering this Langevin description, we expect that the MFT formalism allows to describe other quantities for coherent light aside from intensity correlations. One such example is the calculation of current fluctuations. For the KMP process, under the AP assumption, the CGF was found to be [54]

$$\mu(\lambda) = \begin{cases} -(\sinh^{-1}\sqrt{\Omega})^2 & \text{for } \Omega > 0 \\ +(\sinh^{-1}\sqrt{-\Omega})^2 & \text{for } \Omega < 0, \end{cases}$$

where $\Omega(\lambda, \rho_l, \rho_r) = (1 - e^\lambda)[e^{-\lambda}\rho_l - \rho_r - (e^{-\lambda} - 1)\rho_l\rho_r]$. Moreover, as the AP is valid for the KMP process (see Chapter 3), the universality of current fluctuations discussed in Chapter 4 should be found also for coherent light. Namely, for a quasi-one-dimensional sample, the Fano factor is a universal number.

Another elegant outcome of the MFT formalism is the Gallavotti-Cohen relation [21]. It suggests a relation between a trajectory and its time reversal for a Markovian system, coupled to two reservoirs. The Gallavotti-Cohen relation is a natural result of the MFT [1, 28], where in the language of the LDF, it reads

$$\Phi(J) - \Phi(-J) = J \int_{\rho_l}^{\rho_r} d\rho \frac{D(\rho)}{2\sigma(\rho)}. \quad (5.16)$$

This can be easily seen in the case where the AP applies. The Euler-Lagrange equation (3.5) admits the same density profile for both J and $-J$. Therefore,

$$\Phi(J) - \Phi(-J) = \int dx \left\{ \frac{[J + D\partial_x\rho]^2}{2\sigma} - \frac{[-J + D\partial_x\rho]^2}{2\sigma} \right\}$$

which implies (5.16).

The Gallavotti-Cohen relation generalizes the Einstein relation for systems completely out-of-equilibrium; namely for $J \rightarrow J_s$ and for $\rho_r \rightarrow \rho_l$, (5.16) reduces to the Einstein relation (which can be shown by presenting (5.16) in the CGF formalism and expanding the CGF to second order in λ for a small density gradient). We have seen that the MFT allows to describe fluctuations

⁶The short range term was actually missed in the original paper [45] and later identified in [53].

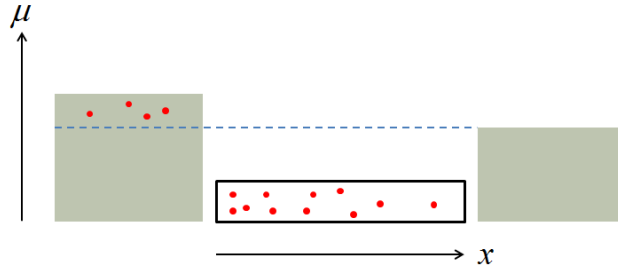


Figure 5.1: Electronic transport through a disordered conductor (schematic). A potential drop causes a shift in the Fermi level (dashed blue line) of the left reservoir. Thus free electrons flow through the system from the left lead (reservoir) to the right lead.

of coherent light in disordered medium. Therefore, the Gallavotti-Cohen relation must manifest itself for coherent light as well. This is both a beautiful and a puzzling result. It suggests a time reversal property for the propagation of coherent light in disordered medium at the microscopic level. However, as the Gallavotti-Cohen relation generalizes the Einstein relation and fluctuation-dissipation theorem, a few puzzling questions arise. The concept of Einstein relation (quantum or classical), imply a connection between an equilibrium and a slightly out-of-equilibrium states of a system. For coherent light, there is no concept of “slightly out-of-equilibrium”. Furthermore, usually to achieve a slightly out-of-equilibrium state, one may apply a field that couples to the particles creating the current. For light propagation in turbid (scattering) media, there is no notion of applied field dragging the medium out of equilibrium. Moreover, the Einstein relation (5.1) suggests that the diffusion and conductivity are related by the charge. For light, there is no such charge. It is still an open and ongoing problem.

5.3.2 Electron Transport Through a Disordered Conductor and the SSEP

The second example we wish to study here is the current fluctuations of electron transport through a disordered conductor, produced by an applied voltage drop. The disordered conductor is coupled to two leads with a voltage drop V (Figure 5.1). The classical Johnson-Nyquist noise formula gives a good description of current fluctuations due to thermal fluctuations. However, at low temperature thermal fluctuations are small and the main contribution to noise is from the discreteness of the electrons, quantum fluctuations and from the randomness of the disorder.

We consider a diffusive quasi-one-dimensional disordered wire, of size L^7 ,

⁷Typically of the order of a micron.

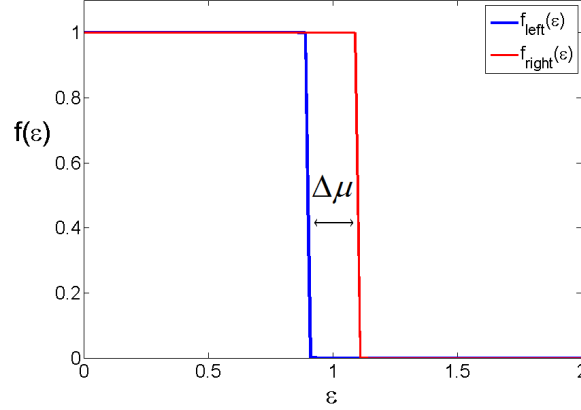


Figure 5.2: The Fermi-Dirac distribution function for the two reservoirs with a chemical potential gradient $\Delta\mu$. It is easy to see that for a small chemical potential gradient, there is a narrow energy band of electrons that contribute to the transport. Here we choose the left (right) chemical potential to be $\mu_l = 0.9, \mu_r = 1.1$ such that $\Delta\mu = 0.2$ with temperature $k_B T \rightarrow 0$ in arbitrary energy units.

small enough such that the electron-electron Coulomb interaction may be disregarded. Namely, the diffusion time $\tau_d \sim \frac{l_e^2}{D}$ is small compared to the electron-electron elastic time τ_{ee} ⁸, where it is understood that for a diffusive behavior $l_e \ll L$. We also require that the wire length is short compared to the coherence length. In these systems the Fano factor, i.e. the ratio between shot noise and current takes the value $F = 1/3$ irrespective of the nature of the disorder or the shape of the wire.

Since we are in the diffusive regime, the steady state current of electrons is induced by the chemical potential gradient at the leads, due to the potential drop. One can also express the steady state current \mathbf{J} using Fick's law, $\bar{\mathbf{J}} = -D\nabla\bar{\rho}(\mathbf{r})$ where ρ is the density of the electrons in the metal, $D = \frac{l_e v_e}{d}$ is the diffusion constant and $\bar{\cdot}$ denotes averaging with respect to the disorder realization. Here, the diffusion coefficient is independent of the distribution, where v_e is the group velocity of the electrons. Before addressing the fluctuations, let us discuss the boundary conditions on the leads. The electrons at the leads of the conductor are at equilibrium. Then, the electronic distribution is the Fermi-Dirac distribution. For $k_B T/eV \rightarrow 0$, the Fermi-Dirac distributions of the two leads are different only for a small energy band (see Figure 5.2). Therefore, only electrons belonging to this energy band contribute to the transport, with distribution $f_l = 1, f_r = 0$ at the left and right leads. The density of electrons at energy ϵ , is given by $\rho_\epsilon = f_\epsilon g_\epsilon$, where g_ϵ is the density of states.

⁸For systems below τ_{ee} , the Coulomb interaction gives negligible changes to the trajectory of the electrons.

It is useful to consider the steady state current using the distribution function gradient, namely $\mathbf{J} = -\tilde{D}\nabla f(\mathbf{r})$ as g_ϵ is spatially independent to a good approximation, and where $\tilde{D} = Dg_\epsilon$. Next, we wish to consider fluctuations. The fluctuations over small scales due the different disorder realizations, much like intensity fluctuations of coherent light, can be considered through a Langevin approach in the form of extraneous currents $\mathbf{j}_{ext}(\mathbf{r})$

$$\mathbf{J}(\mathbf{r}) = -\tilde{D}\nabla f(\mathbf{r}) + \mathbf{j}_{ext}(\mathbf{r}), \quad (5.17)$$

where the $\overline{\mathbf{j}_{ext}(\mathbf{r})} = 0$ follows the steady state current. We consider the correlator of the random extraneous fluxes is given by $\overline{\mathbf{j}_{ext}(\mathbf{r})\mathbf{j}_{ext}(\mathbf{r}')^T} = \delta_{ij}\sigma(f)\delta(\mathbf{r}-\mathbf{r}')$ for $|\mathbf{r}-\mathbf{r}'| \gg l_e$, where i, j denote the spatial directions and $\sigma(f) \propto f(1-f)$. This conductivity is conjectured as the simplest way to support the Pauli exclusion [2]. It should be noted that detailed microscopic calculations do not fully agree with this conjectured conductivity [55]. In the same manner as for coherent light, the idea behind the Langevin formalism, is that the current and densities resulting from random interference of the electron wave-function scattered by the randomly distributed scatterers can be grouped to microscopic fluctuations for $|\mathbf{r}-\mathbf{r}'| < l_e$ and diffusive fluctuations for $|\mathbf{r}-\mathbf{r}'| > l_e$. From this approach, one can obtain the current fluctuations for this electronic transport.

In the language of the MFT, this process has the same macroscopic dynamics as the SSEP. Solving the Euler-Lagrange equation (3.5) (or Hamilton's equations (3.14)) for our D and σ , one can find for our boundary conditions [40, 54]

$$\mu(\lambda) \propto \left(\sinh^{-1} \sqrt{e^\lambda - 1}\right)^2. \quad (5.18)$$

The CGF obtained here for the SSEP, matches exactly to the CGF of electron transport obtained in various methods [49, 56]⁹. We note that this classical description was already realized in [40, 2]. From (5.18), it can be verified that the Fano factor value is indeed 1/3. The universality of current fluctuations obtained in Chapter 4, implies that the value of the Fano factor is independent of the geometry of the conductor. This remarkable observation is indeed found both theoretically and experimentally (see [44, 49] and references within for a detailed discussion). For higher order cumulants, additional effects must be taken into account [55].

Again, we have seen that the MFT formalism allows to describe a mesoscopic system. It is natural to assume as before that the distribution spatial correlations can be successfully described by the MFT approach as well. For the constant diffusion and quadratic conductivity, the correlations are given by the simple form presented in Section 5.2 by (5.11), (5.12) and (5.14).

Also, it was noticed that for a small but non-zero temperature, the CGF maintains the symmetry (see [49] Chapter 10.4)

$$\mu(\lambda) = \mu\left(-\lambda + \frac{eV}{T}\right). \quad (5.19)$$

⁹Apart from a eVg_D prefactor, with $g_D = e^2vD/L$ the mean conductance of the system, and where v is the density of states, integrated over the cross section of the sample.

In the language of the MFT, this is the expression obtained by the Gallavotti-Cohen relation for the SSEP (see [28] Section 12), namely

$$\mu(\lambda) = \mu \left(-\lambda - \log \frac{f_l}{1-f_l} + \log \frac{f_r}{1-f_r} \right). \quad (5.20)$$

Since at the boundaries, $f_{l,r}$ are taken from the Fermi-Dirac distributions, the main contribution for the current is around energy $\epsilon = \mu/2 = eV/2$. We find $f_l \approx \exp[-eV/2k_B T]$ and $f_r \approx 1 - \exp[-eV/2k_B T]$ for $eV/k_B T \gg 1$. From (5.20) and the values of $f_{l,r}$ we recover (5.19). The MFT description is therefore found to be appealing for electronic transport as it successfully captures the physics of current fluctuations as well as help to identify and uncover the origin of the CGF symmetry (5.19) in finite temperature.

5.4 Overview

In this Chapter we have shown that in two cases, the MFT is a convenient tool to describe mesoscopic systems. It was shown also that aside from obtaining known mesoscopic results, new general results such as the universal current fluctuations of Chapter 4 and the Gallavotti-Cohen relation are naturally obtained through the MFT description. These general results are not resulting from a unique microscopic symmetry, or the quantum statistics of the mesoscopic system, but are rather general. Moreover, we propose that the MFT can be used to probe other mesoscopic systems, when a diffusive description of the system in terms of the diffusion and the conductivity is available. This allows for a much easier coarse grained mathematical formalism than the usual microscopic and phenomenological mesoscopic description.

It is interesting to note that any outcome resulting of the MFT formalism, depends only on the diffusion and conductivity as well as on the constraints of the system, i.e. boundary conditions, initial conditions, conservation rules etc. Therefore, quantities such as current fluctuations cannot give new insights on the physics of a system. All the information is already stored in the first two cumulants (albeit for any possible boundary conditions). While measuring the diffusion and conductivity is usually simple experimentally, measuring the higher cumulants, especially in mesoscopic systems, is hard. Therefore, an immediate conclusion from the MFT description is that trying to experimentally measure high cumulants of the current is at best an indirect and a hard approach to extract information about the physics of the system. Moreover, microscopic details tend to be washed out in such measurements, as the success of the MFT clearly shows.

Chapter 6

Summary

In this Thesis we presented three major results. In Chapter 3, we have given a sufficient and necessary condition to the validity of the AP assumption and analyzed the possibility of breakdown of the AP assumption using thermodynamic tools of phase transitions. In Chapter 4, we have shown that under the AP assumption, current fluctuations become universal, namely it depends on the geometry of the system only by a multiplicative geometrical factor which is the effective capacitance of the system. In Chapter 5, we have shown that the MFT is a useful description for transport in disordered quantum systems. This allows to understand such quantum systems from a coarse grained viewpoint and to deduce general (model independent) properties such as the ones introduced in previous chapters.

From a chronological point of view, it was known that the CGF of the SSEP in $1d$ was identical to that of the electronic transport. In mesoscopic physics, the universality of current fluctuations was known for some time. This led for the search for such universality in the MFT (which preceded the results of Chapter 3). Then, in order to address the MFT - mesoscopic correspondence in a formal way, it was necessary to understand whether the AP assumption is useful for system other than the SSEP.

Appendix A

Numerical Methods

It is intuitively understandable that calculating the current fluctuations of a system requires probing rare events, which are, as described by the MFT, exponentially unlikely. Therefore, it is generally impossible to find through exact methods the current fluctuations. Instead of trying to do that, we limit ourselves to trying to extract as many cumulants as we possibly can. Recall that the cumulants are extracted from the CGF,

$$\frac{\langle Q^n \rangle_C}{t} = \left. \frac{\partial^n \mu(\lambda)}{\partial \lambda^n} \right|_{\lambda=0},$$

where $\langle Q^n \rangle_C$ is the n -th cumulant. In the last section, we have shown that the CGF for some arbitrary graph, is the same as for a linear chain of sites, up to an effective conductance. One can rewrite this as $\mu_G(\lambda) = \mu_1(\lambda, L^*)$, where L^* is the effective length of the system. Therefore, it will be convenient to compare ratios of cumulants to get rid of this factor. In this case, it is to be understood that for large systems (where the MFT is valid), we expect that the cumulant ratios are universal. We will see that this is indeed the case, but only for $L^* \gg 1$, as the graph can store many vertices, but has a small effective length. In that case, it is to be expected that the exact solution and the MFT solution differs[40].

There are a number of methods to numerically obtain the cumulants of SSEP. The method of choice here is the one portrayed in the appendix of [57]. The following method advantage is in its robustness; it can easily be adjusted to any graph, however it may be connected to the two (or more) reservoirs. Although [57] shows only how to calculate the first two cumulants of SSEP for source & drain, it can easily be extended to obtain any higher cumulants and to account for different reservoir densities.

The SSEP can be described by a master equation, evolving the probability to observe a configuration of particles in the L system sites. Due to the particle-hole symmetry of the SSEP, it is possible to map the master equation to an equilibrium process described by a Hamiltonian that operates on L spatially fixed spin $\frac{1}{2}$ particles. The CGF inherits a free energy form, and allows to extract

the cumulants via a set of L^n linear equations (where n represents the cumulant number). As the problem becomes harder for large L and for large n , we can only extract the first three cumulants for the SSEP¹.

Here, we consider the simple case of $\rho_a = 1$ and $\rho_b = 0$, namely the system is coupled to a source and a drain. In order to solve the first cumulant (the current) one must solve the set of linear equations

$$-k_{i,S} = \sum_{j(i)} T_j - k_i T_i \quad (\text{A.1})$$

for any i . k_i counts the number of neighbors a site i has on the graph plus the number of connections to the reservoirs. $k_{i,S}$ counts the number of bonds connecting the site i directly with the source. The summation over $j(i)$ means running over all the neighbors j of the site i in the graph, and finally $T_i = T_i(\lambda = 0)$ here denotes the steady state occupation of the site i . The graph sets k_i and $k_{i,S}$ so all the T_i 's are extracted from the simulation. After obtaining T_i , one can simply plug it in

$$I = \sum_{i \in \mathcal{S}} (1 - T_i) \quad (\text{A.2})$$

to obtain the current, where the sum runs over all the sites i connected to the source ($i \in \mathcal{S}$).

The ratio between the second cumulant to the first cumulant is known as the Fano factor, which is simply the noise to signal ratio. It is given by

$$F = 1 - \frac{2 \sum_{i \in \mathcal{S}} T'_i}{\sum_{i \in \mathcal{S}} (1 - T_i)}, \quad (\text{A.3})$$

where $T'_i = \partial_\lambda T_i(\lambda = 0)$, are obtained from the two following sets of equations:

$$\begin{cases} \sum_{l(j), l \neq i} U_{il} + \sum_{l(i), l \neq j} U_{jl} - (k_i + k_j - 2d_{ij}) U_{ij} = -k_{j,S} T_i - k_{i,S} T_j & i \neq j \\ \sum_{l \in \mathcal{S}} (U_{li} - T_l T_i) = \sum_{j(i)} T'_j - k_i T'_i. \end{cases} \quad (\text{A.4})$$

In the first set of Eq.(A.1), d_{ij} counts the number of bonds between sites i and j . $U_{ij} = U_{ij}(\lambda = 0)$ is the two point correlation function at sites i, j , where if $i = j$ then U_{ii} is defined² to be $2T_i - 1$. So, after obtaining all the T'_i 's from Eq.(A.1), one needs to solve the first set in Eq.(A.4) to obtain all the U_{ij} 's, and then use them in the second set of Eq.(A.4) to obtain all the T'_i . Then, from (A.3) one can obtain the Fano factor.

The second Fano factor is the ratio between the third cumulant to the second. It can be obtained by solving

$$\begin{aligned} & U_{ij} (k_{j,S} + k_{i,S} + \mu'(0)) - (k_{j,S} T_i + k_{i,S} T_j + k_{j,S} T'_i + k_{i,S} T'_j) \\ & = \\ & \sum_{m(j), m \neq i} U'_{im} + \sum_{m(i), m \neq j} U'_{jm} - U'_{ij} \{k_i + k_j - 2d_{ij}\} \end{aligned} \quad (\text{A.5})$$

¹The cumulants must also be evaluated successively through a hierarchy of equations.

²This is a matter of convenience in notation

and then solving

$$\mu''(0)T_i + 2\mu'(0)T'_i - \sum_{l \in S} (2T'_i - 2U'_{il} + T_i - U_{il}) = \sum_{j(i)} T''_j - k_i T''_i \quad (\text{A.6})$$

to obtain

$$F_2 = \frac{\sum_{l \in S} (1 - T_l - 3T'_l - 3T''_l)}{\sum_{l \in S} (1 - T_l - 2T'_l)}. \quad (\text{A.7})$$

We have also searched for the first two cumulants in the case where the densities of the reservoirs are not 0 and 1. In this case, a more general set of equations is derived if one sets a general $\alpha, \beta, \gamma, \delta$ which gives for the SSEP $\rho_a = \frac{\alpha}{\alpha+\gamma}$ and $\rho_b = \frac{\delta}{\beta+\delta}$. One observes then that Eq.(A.2) and Eq.(A.3) are reformed to

$$\begin{cases} \bar{I} = \alpha \sum_{i \in A} (1 - T_i) - \gamma \sum_{i \in A} T_i \\ \bar{F} = 1 - 2 \frac{(\alpha+\gamma) \sum_{i \in A} T'_i - \gamma \sum_{i \in A} T_i}{\alpha \sum_{i \in A} (1 - T_i) - \gamma \sum_{i \in A} T_i}. \end{cases} \quad (\text{A.8})$$

To obtain T_i, T'_i and U_{ij} one must solve the set

$$\left\{ \begin{array}{l} 1) \sum_{j(i)} T_j - (k_i + (\alpha + \gamma - 1) k_{i,A} + (\beta + \delta - 1) k_{i,B}) T_i = -\alpha k_{i,A} - \delta k_{i,B} \\ 2) \sum_{j(l)} T'_j - (k_i + (\alpha + \gamma - 1) k_{i,A} + (\beta + \delta - 1) k_{i,B}) T'_i \\ \quad = \alpha \sum_{i \in A} (U_{il} - T_l T_i) - \gamma (\sum_{i \in A} (T_l T_i - U_{il}) + k_{l,A} (2T_l - 1)) \\ 3) \begin{aligned} & \sum_{j(m), j \neq l} (U_{lj} - U_{lm}) + \sum_{j(l), j \neq m} (U_{jm} - U_{lm}) \\ & + \alpha \{k_{m,A} (T_l - U_{lm}) + k_{l,A} (T_m - U_{lm})\} - \gamma \{k_{m,A} U_{lm} + k_{l,A} U_{lm}\} \\ & \delta (k_{m,B} (T_l - U_{lm}) + k_{l,B} (T_m - U_{lm})) - \beta (k_{m,B} + k_{l,B}) U_{lm} \end{aligned} = 0. \end{array} \right. \quad (\text{A.9})$$

To conclude this section, if one has a graph of L sites, one must solve a set of order $\sim L^n$ linear equations to obtain any cumulant of order higher than one. This makes the simulation run efficiently only on small graphs, luckily, the MFT limit seems to be achieved for relatively small number of sites.

Bibliography

- [1] L. Bertini, A. De Sole, D. Gabrielli, G. Jona-Lasinio, and C. Landim. *Rev. Mod. Phys.*, 87:593, 2015.
- [2] A. N. Jordan, E. V. Sukhorukov, and S. Pilgram. *J. Math. Phys.*, 45:4386, 2004.
- [3] C. Arita, P.L. Krapivsky, and K. Mallick. *Phys. Rev. E*, 90:052108, 2014.
- [4] P. C. Martin, E. D. Siggia, and H. A. Rose. *Phys. Rev. A*, 8:423, 1973.
- [5] L. Bertini, A. De Sole, D. Gabrielli, G. Jona-Lasinio, and C. Landim. *Phys. Rev. Lett.*, 87:040601, 2001.
- [6] D. Gabrielli L. Bertini, A. De Sole and C. Landim. *J. Stat. Phys.*, 107:635, 2002.
- [7] L. Bertini, A. De Sole, and D. Gabrielli. *Mathematical Physics, Analysis and Geometry*, 6:231, 2003.
- [8] C. Kipnis, C. Marchioro, and E. Presutti. *J. Stat. Phys.*, 27:65, 1982.
- [9] K. Saito and A. Dhar. *Phys. Rev. Lett.*, 107:250601, 2011.
- [10] L. Bertini, A. De Sole, D. Gabrielli, G. Jona-Lasinio, and C. Landim. *Journal of Statistical Mechanics: Theory and Experiment*, page P07014, 2007.
- [11] L. Bertini, A. De Sole, D. Gabrielli, G. Jona-Lasinio, and C. Landim. *cond-mat arXiv*, 0705:2996, 2007.
- [12] L. Bertini, A. De Sole, D. Gabrielli, G. Jona-Lasinio, and C. Landim. *J. Stat. Phys.*, 135:857, 2009.
- [13] L. Bertini, A. De Sole, D. Gabrielli, G. Jona-Lasinio, and C. Landim. *Journal of Statistical Mechanics: Theory and Experiment*, L11001, 2010.
- [14] L. Bertini, A. De Sole, D. Gabrielli, G. Jona-Lasinio, and C. Landim. *J. Stat. Phys.*, 149:773, 2012.
- [15] L. Bertini, A. De Sole, D. Gabrielli, G. Jona-Lasinio, and C. Landim. *Phys. Rev. Lett.*, 110:020601, 2013.

- [16] D. Kambly, C. Flindt, and M. Büttiker. *Phys. Rev. B*, 83:075432, 2011.
- [17] Y. Baek, Y. Kafri, and V. Lecomte. *Journal of Statistical Mechanics: Theory and Experiment*, P053203, 2016.
- [18] O. Hirschberg, D. Mukamel, and G.M. Schütz. *Journal of Statistical Mechanics: Theory and Experiment*, P11023, 2015.
- [19] H. Touchette. *Physics Reports*, 478:1, 2009.
- [20] T. Bodineau and B. Derrida. *Phys. Rev. Lett.*, 92:180601, 2004.
- [21] G. Gallavotti and E. G. D. Cohen. *Phys. Rev. Lett.*, 74:2694, 1995.
- [22] P. I. Hurtado and P. L. Garrido. *J. Stat. Mech.*, P02032, 2009.
- [23] P. Hurtado and P. Garrido. *Phys. Rev. Lett.*, 102:250601, 2009.
- [24] P. I. Hurtado and P. L. Garrido. *Phys. Rev. E*, 81:041102, 2010.
- [25] P. I. Hurtado, C. Pérez-Espigares, J. J. del Pozo, and P. L. Garrido. *Proceedings of the National Academy of Sciences of the United States of America*, 108:7704, 2011.
- [26] J. J. Pozo P. I. Hurtado, C.P. Espigares and P. L. Garrido. *J. Stat. Phys.*, 154:214, 2013.
- [27] M. Gorissen and C. Vanderzande. *Phys. Rev. E*, 86:051114, 2012.
- [28] B. Derrida. *Journal of Statistical Mechanics: Theory and Experiment*, P07023, 2007.
- [29] T. Bodineau and B. Derrida. *C. R. Physique*, 8:540, 2007.
- [30] T. Bodineau, B. Derrida, V. Lecomte, and F. van Wijland. *J. Stat. Phys.*, 133:1013, 2008.
- [31] L. Zarfaty and B. Meerson. *Journal of Statistical Mechanics: Theory and Experiment*, 033304:1, 2015.
- [32] P. I. Hurtado and P. L. Garrido. *Phys. Rev. Lett.*, 107:1, 2011.
- [33] C. Espigares, P. Garrido, and P. Hurtado. *Phys. Rev. E*, 87:032115, 2013.
- [34] C. Appert-Rolland, B. Derrida, V. Lecomte, and F. van Wijland. *Phys. Rev. E*, 78:021122, 2008.
- [35] H. B. Callen. *Thermodynamics and an Introduction to Thermostatistics*. John Wiley, 2nd edition, 1960.
- [36] Luca Peliti. *Statistical Mechanics in a Nutshell*. Princeton university press, 2011.

- [37] L. Bertini, A. De Sole, D. Gabrielli, G. Jona-Lasinio, and C. Landim. *J. Stat. Phys.*, 123:237, 2006.
- [38] O. Shpielberg and E. Akkermans. *cond-mat arXiv, to be published in Phys. Rev. Lett.*, 05254:1510, 2015.
- [39] Kirone Mallick. *Physica A: Statistical Mechanics and its Applications*, 418:17, 2015.
- [40] B. Derrida, B. Douçot, and P.-E. Roche. *J. Stat. Phys.*, 115:717, 2004.
- [41] L. Bertini, A. De Sole, D. Gabrielli, G. Jona-Lasinio, and C. Landim. *Phys. Rev. Lett.*, 94:030601, 2005.
- [42] T. Bodineau and B. Derrida. *J. Stat. Phys.*, 123:277, 2006.
- [43] E. Akkermans, T. Bodineau, B. Derrida, and O. Shpielberg. *Europhys. Lett.*, 103:20001, 2013.
- [44] E. Akkermans and G. Montambaux. *Mesoscopic Physics of Electrons and Photons*. Cambridge University Press, 2007.
- [45] A. Yu. Zyuzin and B. Z. Spivak. *Sov. Phys. JETP*, 1006:560, 1987.
- [46] C. H. L. Quay, D. Chevallier, C. Bena, and M. Aprili. *Nature Physics*, 9:84, 2013.
- [47] S.-a. Biehs, E. Rousseau, and J.-J. Greffet. *Phys. Rev. Lett.*, 105:234301, 2010.
- [48] K. Saito and A. Dhar. *Phys. Rev. Lett.*, 99:1, 2007.
- [49] A. Kamenev. *Field theory of non-equilibrium systems*. Cambridge University Press, 2011.
- [50] H. Spohn. *Large Scale Dynamics of Interacting Particles*. Springer, 2nd edition, 1992.
- [51] T. Sadhu, S. N. Majumdar, and D. Mukamel. *Phys. Rev. E*, 84:051136, 2011.
- [52] E. Landau, L. Lifshitz. *Mechanics*. Pergamon Press, 3rd edition, 1976.
- [53] R. Pnini and B. Shapiro. *Phys. Rev. B*, 39:6986, 1989.
- [54] A. Imparato, V. Lecomte, and F. van Wijland. *Phys. Rev. E*, 80:011131, 2009.
- [55] E. Akkermans. *private communication*.
- [56] Hyunwoo Lee, L.S. Levitov, and A.Yu Yakovets. *Phys. Rev. B*, 51:4079–4083, 1995.
- [57] C. Groth, J. Tworzydło, and C. Beenakker. *Phys. Rev. Lett.*, 100:176804, 2008.

אשתמש בתנאי זה, כדי להראות ש"עקרון החיבוריות" מתקיים בשני מודלים בעלי ערך לקהילה. בנוסף, אציג פיתוח של כלים נומריים, המאפשרים לחשב האם ומתי אנו נראה מעבר פאזה דינמי המבשר על שבירה של "עקרון החיבוריות". מעבר לכך, אציג בתיזה זאת את האוניברסליות של פלוקטואציות הזרם לגבי מערכות עם גיאומטריה כלשהי, תוך הסתמכות על "עקרון החיבוריות". הגודל האופייני השני עליו נדבר הוא קורלציות של פונקציית הצפיפות מחוץ לשיווי משקל. בשיווי משקל, רחוק ממעבר פאזה, פונקציית הקורלציה דועכת אקספוננציאלית. לעומת זאת, במערכות הרחוקות משיווי משקל, פונקציית הקורלציה דועכות כמו חוק חזקה. כלומר, אנו מצפים למצוא קורלציות ארוכות טווח. בעזרת תוצאות ידועות של תורת הפלוקטואציות המקרוסקופיות, אראה התאמה מלאה בין מודלים קלאסיים למודלים של מערכות מזוסקופיות עם אי-סדר. מכך נלמד, כי תורת הפלוקטואציות המקרוסקופיות מאפשרת לנו לדון במערכות סטוכסטיות, קלאסיות או קוונטיות.

תקציר

תרמודינמיקה ומכניקה סטטיסטית עוסקות במידול של מערכות בעלות דרגות חופש רבות, הנמצאות בשיווי משקל. כבר יותר ממאה שנה הרעיונות שפותחו עבור מערכות בשיווי משקל, עוזרים להבין את העולם סביבנו ונוגעים בכל תחומי מדעי הטבע. במערכות בשיווי משקל התרמודינמיקה נותנת לנו יכולת חיזוי לגדלים ממוצעים בלבד, וקושרת בין הגדלים התרמודינמיים כמו לחץ, טמפרטורה ונפח, בעזרת משוואות מצב. מכניקה סטטיסטית מספרת לנו בעזרת חישוב מיקרוסקופי, שבמערכות גדולות המצב הממוצע הוא בדרך כלל גם המצב המסתבר ביותר. מעבר לכך, בליבה של המכניקה הסטטיסטית נטועה ההנחה כי ספירה של המצבים האנרגטיים האפשריים של המערכת מספיקה בכדי לתת ביטוי לגדלים התרמודינמיים. כלומר, אין כלל חשיבות לדינמיקה של קצבי המעבר בין המצבים האנרגטיים.

למרות ההצלחה הזאת, ההתקדמות בהבנה של תהליכים מחוץ לשיווי משקל הייתה מועטה, ובדרך כלל התמקדה בתהליכים, שההפרה של שיווי משקל תרמודינמי בהם קטנה. הסיבה להתקדמות המועטה היא, שבניגוד לפיסיקה בשיווי משקל, הדינמיקה חשובה מאוד במערכות מחוץ לשיווי משקל; הזמן משחק תפקיד קריטי וישנם תמיד זרמי הסתברות, שגורמים למערכת לעבוד בין המצבים השונים בצורה לא טריוויאלית.

תורת הפלוקטואציות המקרוסקופיות מציעה התקדמות ממשית במחקר של מערכות דיפוזיביות מחוץ לשיווי משקל מנקודת מבט מקרוסקופית, בדומה לתרמודינמיקה. הוכח, שהיא מצליחה לשחזר תוצאות עבור מודלים פשוטים ופתורים של תהליכים מחוץ לשיווי משקל. הרעיון מאחורי תורת הפלוקטואציות המקרוסקופיות הוא, שכאשר הדינמיקה היא דיפוזיבית, אפשר לחלק את המערכת לתת-מערכות מזוסקופיות רבות, כך שכל אחת מהן נמצאת בשיווי משקל מקומי וניתנת לתיאור על-ידי גדלים ממוצעים. בעזרת שימוש בידע שנצבר על מערכות המפרות מעט את שיווי המשקל התרמודינמי, ותפירת המערכות המזוסקופיות חזרה למערכת מקרוסקופית, תורת הפלוקטואציות המקרוסקופיות נותנת תחזיות לגבי ההתפתחות של המערכת בזמן ובמרחב.

בעבודת מחקר זאת אני אתמקד במערכות דיפוזיביות שנשמרות מחוץ לשיווי משקל על-ידי שני אמבטים של חלקיקים, כאשר צפיפות חלקיקים שונה בכל אמבט – כל זאת במסגרת התיאור של תורת הפלוקטואציות המקרוסקופיות. ארחיב על שני גדלים שמאפיינים מערכות מחוץ לשיווי משקל.

הגודל האופייני הראשון, פלקטואציות של הזרם, מאפשר לקבל אינטואיציה על הפיסיקה ששולטת במערכת מתוך המידע על הרעש הסטטיסטי של הזרם. במערכות גרניות, חישוב של פלוקטואציות הזרם אינו דבר טריוויאלי אנליטית ואפילו נומרית. אולם, נחוש חכם, הידוע בשם "עקרון החיבוריות", מאפשר לקבל ביטוי אנליטי עבור פלקטואציות של זרמים. אני אראה כי ניתן לפרש שבירה של "עקרון החיבוריות" כמעבר פאזה דינמי, ועל-ידי כך ניתן יהיה לדון בשבירה של "עקרון החיבוריות" בעזרת עקרון לה-שטלייה המפורסם מתרמודינמיקה. בתיזה זאת אציג תנאי מספיק והכרחי עבור הקיום של "עקרון החיבוריות".

המחקר נעשה בהנחיית פרופסור אריק אקרמן בפקולטה לפיסיקה

אני מודה לטכניון על התמיכה הכספית הנדיבה בהשתלמותי

**מכניקה סטטיסטית מחוץ לשיווי משקל:
רשתות חשמליות ועקרון האדיטיביות**

חיבור על מחקר

לשם מילוי חלקי של הדרישות לקבלת התואר דוקטור
לפילוסופיה

אוהד שפילברג

הוגש לסנט הטכניון - מכון טכנולוגי לישראל

סיוון, 5776 חיפה יוני, 2016

**מכניקה סטטיסטית מחוץ לשיווי משקל:
רשתות חשמליות ועקרון האדיטיביות**

אוהד שפילברג